CEREBRAL PALSY MOTION ANALYSIS USING A WEARABLE ACTIVITY TRACKING DEVICE AND HUMANOID ROBOT

Nicholas J. Cooney

Master of Research in the Faculty of Science and Engineering

School of Engineering
Macquarie University

October 25, 2019

Supervisor: Dr. Atul Singh Minhas

ACKNOWLEDGEMENTS

I would like to acknowledge my family, who have always provided a great deal of support to me in all of my life choices. I would also like to acknowledge Dr. Atul Singh Minhas for his guidance and encouragement throughout the project. I would like to thank Morgan Wheatley for his help in designing and manufacturing the 3D-printed case used in this study. I acknowledge the research participants who gave their time to assist me in the collection of human movement data.

STATEMENT OF CANDIDATE

I, Nicholas Cooney, declare that this report, submitted as part of the requirement for the award of Master of Research in the Faculty of Science, Macquarie University, is entirely my own work unless otherwise referenced or acknowledged. This document has not been submitted for qualification or assessment at any academic institution.

Ethical approval for the project was granted by the Science & Engineering Subcommittee (reference number 52019575710245).

Student's Name: Nicholas Cooney

Student's Signature: *N. Cooney*

Date: 23/10/19

ABSTRACT

Wearable devices for human activity tracking are becoming a commonly used infotainment gadget in daily life. Many commercial devices have emerged for human health and wellness assessment, such as daily physical activity monitoring through step counting or exercise tracking. The popularity of wearables has improved drastically with developments in internet of things (IoT) technologies and the ability to analyse data with cloud-computing. However, wearables have not been fully utilized in the physical activity tracking of disabled people. This is primarily due to the ethical requirements and restrictions imposed when acquiring data from this cohort. In this study, we show that humanoid robots have the potential to be used as a model for the movement and physical activity analysis of disabled people. This will aid in the development of wearable devices capable of providing services to disabled people.

Contents

List of Figures

List of Tables

Chapter 1

Introduction

Wearable devices for physical activity monitoring are becoming increasingly more common. There are many commercially available solutions for individuals who wish to monitor their physical activity, such as smartwatches and fitness trackers from companies like Fitbit, Apple, Samsung and many others. There are also high-end systems available which offer an accurate yet expensive solution to wireless motion tracking, such as the various inertial measurement units (IMUs) from Xsens [1] and the Blue Trident IMU from Vicon [2]. Smartwatches and fitness trackers readily deliver generic metrics that track activity, such as step count and sleep pattern tracking, which are not useful in clinical motion analysis. More advanced data can be accessed by the user, but this is often gated with a membership and recurring fee [3]. Through developer application programming interfaces (APIs), such trackers can be made to deliver some raw sensor data, but limitations on data access rate per hour are generally imposed [4]. Custom-built wearable devices have been proposed and developed which aim to offer a home-based solution for the physical activity monitoring of people with disabilities [5–8]. These custom-built solutions are more suitable for use in physical activity tracking research than the current commercial solutions, for both home-based and in-clinic applications, as they provide cheap and unlimited access to raw sensor data and the ability for edge-computer integration. However, home-based activity monitoring system architectures are not yet ready for general acceptance by healthcare service providers and system developers and are still under active research and development.

Wearable devices have been utilised in clinical research for their ability to provide biomedical, physiological and motion sensing data. Wearables are an extremely powerful technology, offering useful solutions to many health-based problems [9]. Applications include assessment of treatment efficacy [10], home-based rehabilitation [11],

health and wellness tracking [12], and early detection of disorders [13]. A substantial amount of research with motion sensors specifically has been conducted in multiple sclerosis (MS), with a focus on physical activity intensity classification [14].

Cerebral palsy (CP) is a non-progressive brain disorder which causes long-term physical disability resulting in limited movement and mobility [15, 16]. Although the brain injury is non-progressive, due to musculoskeletal pathologies the physical impairments of an individual with CP often do worsen over time. These pathologies include spasticity, muscle weakness and bone deformity [15]. The most common motor disorder in children with CP is spasticity, making spasticity assessment highly important for safe and efficient interventions. Common clinical measures of spasticity include the modified Ashworth scale (MAS), the modified Tardieu scale (MTS) [16], and the pendulum test (PT) [17]. Other common clinical measurement methods for CP include the Gross Motor Function Measure (GMFM), which is used to assess gross motor development in children with CP [18], and instrumental gait analysis, which uses the gait characteristics of an individual to assess motor deficits [17]. The potential for integration of wearables into these various assessment methods has recently been presented in the literature [16, 17, 19–22], but the work done is limited.

A common method used for assessing spasticity is the PT [17] originally described by Wartenberg [23, 24]. The PT uses gravity to provoke the muscle stretch reflex during passive swinging of the lower leg. Characterization of the leg oscillations with electrogoniometry, videography and magnetic sensing devices may provide an objective measure to differentiate between various degrees of spasticity in children with CP. More recently, an accelerometer-based sensing method has been used, which provides versatile, high sensitivity measurements and excellent reliability while being less expensive than other movement analysis systems [17]. The cheap and accurate motion tracking that wearables are able to provide is heavily underutilized in CP research.

The levels of disability severity vary widely across the CP population. Therefore, it is difficult to form a group of CP individuals which can provide us statistically significant data of motion impairments with common characteristics. Besides, stringent ethical approval requirements exist to collect research data from the CP cohort. All these restrictions make research data collection from CP individuals a very difficult and time-consuming process. Humanoid robots may have the potential to model disabled movement, which would make research on disabled motion more accessible. To our knowledge, humanoid robots have not been used as a model for human movement in the literature. This approach is a new opportunity in clinical activity tracking research, and has been studied in this project with use of the Alpha 1 humanoid robot [25].

1.1 Aims and Objectives

The overarching aim of this study is to investigate the efficacy of using humanoid robots as a model for the physical activity analysis of disabled individuals, such as those affected by cerebral palsy. This study has following objectives:

- Develop calibration methods for accurate data collection from a custom-built wearable activity tracking device (WATD).
- Develop pre-processing methods for motion data captured by the WATD.
- Conduct an exhaustive literature review to program the Alpha 1 humanoid robot to act as a model for CP motion and track this motion using the WATD.
- Collect normal and imitated CP movement data from healthy human participants to validate the use of the Alpha 1 robot as a model for CP.

1.2 Organisation of the Thesis

The thesis is organised as follows:

Chapter 1 introduces and provides a background of the research and technology topics relevant to this study. An overview of the current state of wearable devices used commercially and in clinical research is given. CP is introduced, as well as various common assessment methods for the disease, with a focus on the PT. The Alpha 1 humanoid robot is presented as a potential research tool for modelling CP motion. Finally, the aims and objectives of the study are laid out.

Chapter 2 runs through the exhaustive literature review that was conducted to find motion data that could be used to program the Alpha 1 robot. The focus of the literature review is research papers which use wearables in CP research. The search strategy, inclusion criteria and survey results are discussed and a conclusion of the review is given.

Chapter 3 describes the methodology that was used in the current study. The experimental setup is presented, showing the research apparatus and explaining how this equipment was used. Data processing and analysis techniques are then described. Finally, the movement activities that were used in this study are explained.

Chapter 4 presents and discusses the results of the study. First, the effect of device calibration and the 3D-printed case are discussed. After this, the human and robot results from the movement activities are laid out. Finally, the use of the Alpha 1 humanoid robot and WATD are evaluated.

Chapter 5 concludes the study and presents plans for future work with this research.

Chapter 2

Background and Literature Review

2.1 Introduction

CP treatment interventions often include physical rehabilitation to increase mobility and reduce pain [16]. To gauge the severity of CP and assess the effectiveness of treatment, clinical examination combined with gait analysis is commonly used [20]. Several tools can be used in instrumented gait analysis, such as 3D motion capture systems, 2D systems using video cameras with analysis software, or pressure sensitive mats [26]. These measurement systems do not provide an ideal solution. Generally they are non-portable, costly, and must be used in dedicated laboratories due to their bulky nature. Subject preparation, a laboratory environment, and limited space to allow for a natural gait pattern make these gait analysis measurement tools unfavourable for patients [22].

IMUs are widely used in research to track motion. Some researchers have proposed IMUs for gait analysis [22]. IMUs are also proposed for tracking motion during the PT [17]. Usually IMUs consist of at least a 3-axis accelerometer and 3-axis gyroscope, but many are equipped with a 3-axis magnetometer. With the ability to measure movement in 9 separate axes, such IMUs are often called 9 degrees of freedom (9DOF) IMUs. There are many commercial solutions which are cheaply available and compatible with common hobby electronics boards.

The aim of this review is to survey the literature for studies that utilise IMU technology to measure the movement of individuals with CP. From these papers, various angular parameters that define CP motion will be extracted and collated to construct a library of movement data. Using this library, the Alpha 1 humanoid robot [25] will be programmed to model CP movement. Programming the Alpha 1 robot to mimic real

CP motion will make it an invaluable research tool for testing and calibrating novel wearable activity tracking devices. This robot model could also be used in conjunction with wearables to generate massive amounts of motion data to aid in the development of machine learning algorithms to diagnose, classify and treat CP in the future.

2.2 Search Strategy

A search of the literature from January 2000 to October 2019 was conducted using the electronic databases Medline Complete and PubMed through Macquarie University permissions. The search terms aimed to find any articles and papers which were on the topic of cerebral palsy and made use of a 9DOF IMU. In both PubMed and Medline Complete, the search terms used were as follows: "(accelerometer OR gyroscope OR magnetometer) AND cerebral palsy". The reference lists of articles, conference papers, and systematic reviews from the search engines were manually checked in full, except where Macquarie University did not have the relevant permissions to allow access to the full article. Relevant articles were extracted from the database reference lists using the inclusion criteria listed in section 2.3.

2.3 Inclusion Criteria

Inclusion criteria aimed to find journal articles and conference papers that contained any angular motion data relating to the movement of individuals with CP. The survey was not specific to activity type or particular bodily angles. Articles or papers were included if they (1) included only participants of any age with cerebral palsy of any severity; (2) studied any kind of activity or therapy which involved movement of the body, and (3) gave clear and useful numerical data relating to the angular movements of the body. Articles or papers were excluded if they (1) did not include individuals with CP as the sole participant; (2) did not present original data (systematic review papers); (3) were not available as a full text through Macquarie University's licensing permissions; (4) did not look at the movement of study participants, or (5) did not present useful numerical data relating to the angular movements of the body.

2.4 Survey Results

Searches on the Medline Complete and PubMed electronic databases identified 168 records, of which 72 were duplicates. 96 full text articles were assessed for their eligibility. Figure 2.1 summarises the literature survey technique and reasons for exclusions. Of the 86 papers, 8 had useful numerical data relating to the angular movements of the body. 7 are journal papers and 1 is a conference paper.

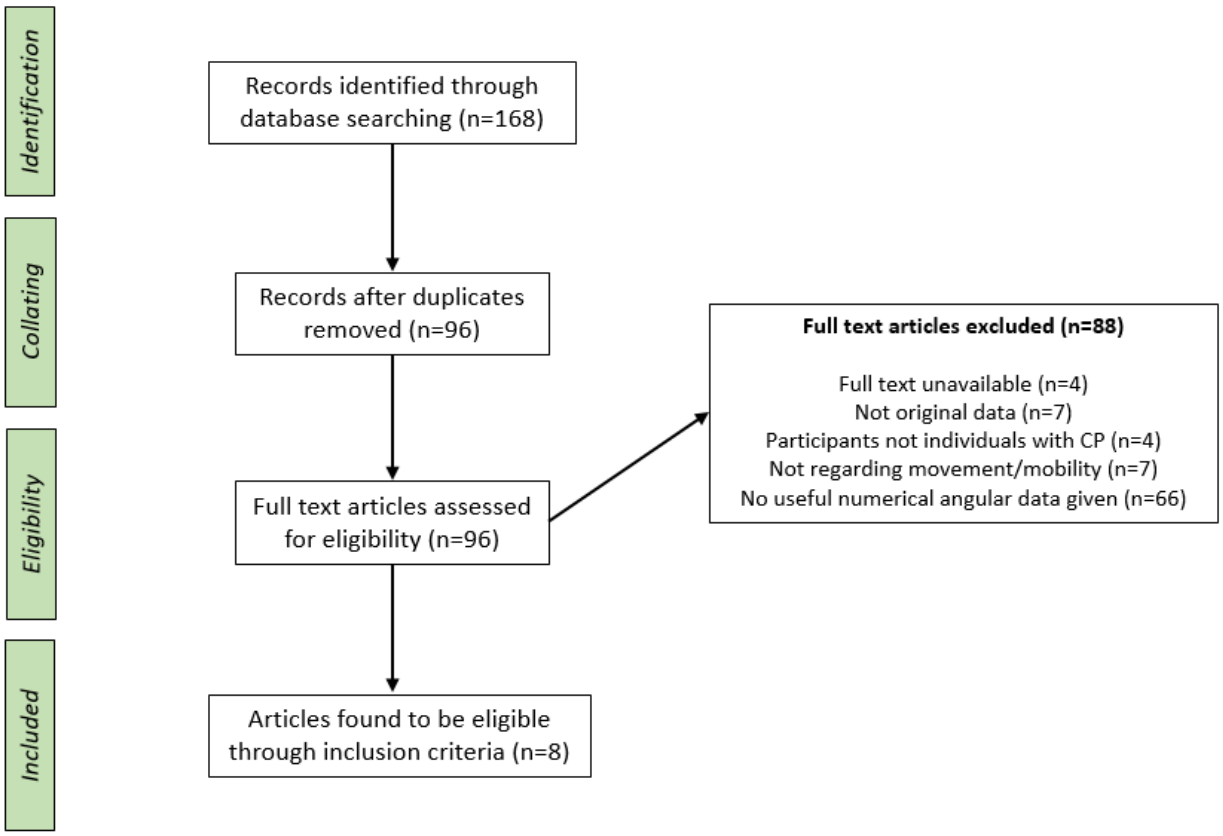

Figure 2.1: Flowchart summarising the literature survey technique and denoting numbers of articles found, included and excluded.

The two electronic databases (PubMed and Medline Complete) returned very similar results and showed the same trend of papers published across time. This can be seen in figure 2.2. All 72 of the records found on PubMed were also found on Medline Complete (termed duplicates in figure 2.1). Medline Complete had an additional 24 unique records, out of which only 1 additional eligible paper was found (out of a total of 8 eligible papers). Figure 2.2 shows the growing trend of using 9DOF IMU modules in research related to CP.

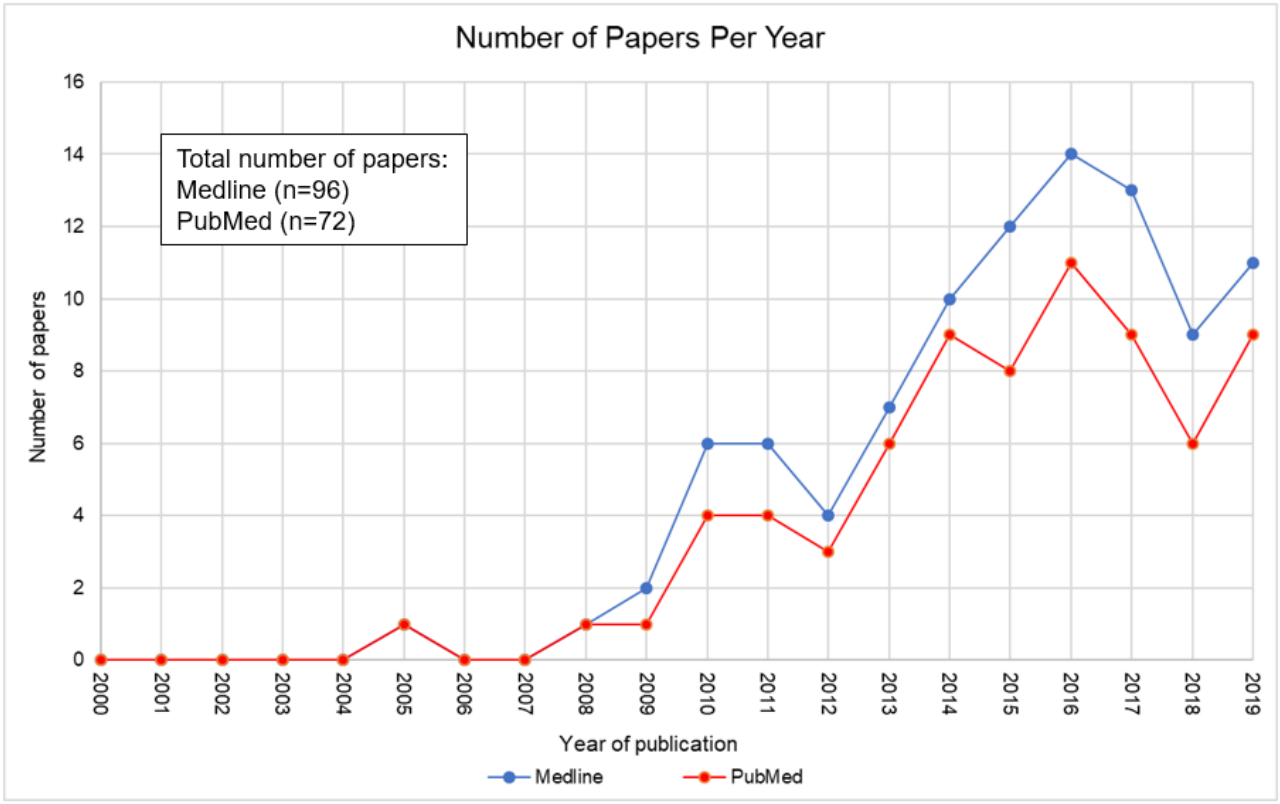

Figure 2.2: A graph displaying the number of papers and the date of publication found in the literature survey. Note that all 72 records found using the PubMed database were also present in the Medline Complete search.

As laid out in the inclusion criteria, papers regarding the movement of individuals with CP were only deemed eligible if clear numerical data relating to the angular movements of the body were given. The 8 eligible papers found through the literature survey are summarised in table 2.2. The papers are all published recently, the earliest being published in 2012. 6 of the 8 papers provide data on various angles of the legs of individuals with CP, with clinical gait analysis being a commonly used research method.

Table 2.1: Summary of the 8 eligible papers found in the literature survey.

Paper Title	Year of Publication	Hardware/ Measurement Equipment	Type and Severity of CP	Part of Body Studied/Sensor Placement	Activity/ Application	Description of Numerical Data
Locomotion and cadence detection using a single trunk-fixed accelerometer: validity for children with cerebral palsy in daily life-like conditions [15]	2019	6 synchronised IMUs (Physilog4®, Gait Up). No magnetometer recordings used.	Gross Motor Function Classification System (GMFCS) I-III.	IMUs were mounted on participants' sternum, lower back, thighs, and shanks.	Clinical gait analysis.	Angular velocity (degrees per second) data from the chest and lower back mounted IMUs is given for 3 different types of CP.
Augmented effects of EMG biofeedback interfaced with virtual reality on neuromuscular control and movement coordination during reaching in children with cerebral palsy [27]	2017	A goniometer was used to measure the angle of participants' elbow.	4 diplegia, 1 hemiplegia, 5 quadriplegia.	The balance control of the elbow joint of individual's with CP was studied.	Arm reaching activity.	Elbow flexion and extension angular ranges of motion are given.
Improving modified Tardieu scale assessment using inertial measurement unit with visual biofeedback [16]	2016	Type of IMU not specified.	Spastic CP.	The movement of the legs was assessed.	Modified Tardieu scale assessment.	Angular range of motion, angle of catch, and spasticity angle during modified Tardieu scale assessment are given.

Paper Title	Year of Publication	Hardware/ Measurement Equipment	Type and Severity of CP	Part of Body Studied/Sensor Placement	Activity/ Application	Description of Numerical Data
The Effect of Ankle-Foot Orthoses on Community-Based Walking in Cerebral Palsy: A Clinical Pilot Study [28]	2016	StepWatch multi-axis accelerometer.	GMFCS I-III, bilateral CP.	The movement of the legs was assessed.	Clinical gait analysis.	Shank to vertical angle data is given for 11 different children with CP.
Validation of Inter-Subject Training for Hidden Markov Models Applied to Gait Phase Detection in Children with Cerebral Palsy [21]	2015	2 IMUs (Xbus Master MTx, Xsens Technologies, Enschede, The Netherlands)	10 hemiplegia.	The movement of the legs was assessed. Sensors were mounted on the foot and shank of the most affected leg.	Clinical gait analysis.	Angular velocity (degrees per second) data from the foot and shank is given.
Quadriceps femoris spasticity in children with cerebral palsy: measurement with the pendulum test and relationship with gait abnormalities [17]	2014	Accelerometer-based system with ZK software during Dynamic Evaluation of Range of Movement (DAROM) and pendulum test. Compact Measuring System for 3D Real-Time Motion Analysis (CMS-HS 3D) with WinGait software during clinical gait analysis.	Spastic CP – 18 hemiplegia, 18 diplegia. GMFCS I-II.	Accelerometers were placed on the shanks.	DAROM, pendulum test, and clinical gait analysis.	Angular data from the DAROM and pendulum test is given.

Paper Title	Year of Publication	Hardware/ Measurement Equipment	Type and Severity of CP	Part of Body Studied/Sensor Placement	Activity/ Application	Description of Numerical Data
The relationship between clinical measurements and gait analysis data in children with cerebral palsy [20]	2013	Range of motion deficit (DROM) angles were measured using an accelerometer-based system with ZK software. Compact Measuring System for 3D Real-Time Motion Analysis (CMS-HS 3D) with WinGait software during clinical gait analysis.	Spastic CP – 18 hemiplegia, 18 diplegia. GMFCS I-II.	The accelerometer was placed on 4 different locations of the leg depending on the DAROM test being undertaken.	DAROM test and clinical gait analysis.	Various leg DROM angles given for the DAROM test. Angle of spasticity also given.
Stability and harmony of gait in children with cerebral palsy [19]	2012	Wearable IMU (FreeSense®), containing an accelerometer and gyroscope.	Spastic CP – 17 hemiplegia. GMFCS I-II.	The IMU was worn on the back, near the body centre of mass.	Clinical gait analysis.	Peak-to-peak angular velocities (PPV) of the sensor during gait in 3 axis directions are given.

2.5 Discussion

The 8 eligible papers can be sorted into 3 groups as listed in table 2.2. Group 1 papers present angular data which may be useful for programming gait motion into the Alpha 1 robot. Group 2 papers present specific angular data sets from various tests, analyses and assessments, as opposed to normal everyday movement. The data from group 2 papers is useful for programming CP movement into the Alpha 1 robot which mimics motion from these specific clinical analyses. Group 3 has only one article; it is set apart from the other 7 papers because it does not study gait or lower body motion.

Table 2.2: Grouping of the 8 eligible papers.

Paper Title	**Year of Publication**	**Group Number**
Locomotion and cadence detection using a single trunk-fixed accelerometer: validity for children with cerebral palsy in daily life-like conditions [15]	2019	1
Augmented effects of EMG biofeedback interfaced with virtual reality on neuromuscular control and movement coordination during reaching in children with cerebral palsy [27]	2017	3
Improving modified Tardieu scale assessment using inertial measurement unit with visual biofeedback [16]	2016	2
The Effect of Ankle-Foot Orthoses on Community-Based Walking in Cerebral Palsy: A Clinical Pilot Study [28]	2016	1
Validation of Inter-Subject Training for Hidden Markov Models Applied to Gait Phase Detection in Children with Cerebral Palsy [21]	2015	1
Quadriceps femoris spasticity in children with cerebral palsy: measurement with the pendulum test and relationship with gait abnormalities [17]	2014	2
The relationship between clinical measurements and gait analysis data in children with cerebral palsy [20]	2013	2
Stability and harmony of gait in children with cerebral palsy [19]	2012	1

The papers in group 1 provide angular data on CP gait. Reference [15] provides 3 CP individuals' shank pitch angular velocity data during gait. This information could be used to set the Alpha 1 robot's legs moving at a speed similar to an individual with CP during gait. Reference [28] provides the shank to vertical angle of children with CP during gait. This is useful data to ensure the Alpha 1 robot's lower legs are positioned correctly at the midstance of the gait. Reference [21] presents a detailed graph of the

foot and shank angular velocity during gait, with the stride broken into progressively more detailed partitions. This data could be used to tune the Alpha 1 robot's stride speed to more closely mimic a typical CP gait. Reference [19] provides peak-to-peak angular velocities in 3 body axis directions (CC: cranio-caudal, LL: latero-lateral, AP: antero-posterior). This data may be useful to compare the Alpha 1 robot's gait stability against, to ensure it is as similar as possible to a typical CP gait.

Papers in group 2 use various tests, analyses and assessments to generate angular data on individuals with CP. Reference [16] uses MTS assessment with both a novel IMU approach and a conventional approach. Exact angle ranges are provided for range of motion, angle of catch, and angle of spasticity of CP individuals during the MTS assessment. This data could be used to mimic the MTS assessment with the Alpha 1. References [17] and [20] provide angular data from the DAROM tests, while reference [17] also looks at the PT. Similarly, this data could be used to program the Alpha 1 to mimic these tests.

Reference [27] is alone in group 3. It is the only paper that is not focused on lower body movement or gait analysis. Reference [27] studies angular elbow flexion and extension ranges of motion in children with CP while seated. This data would be useful to program the Alpha 1 robot to mimic a similar reaching task.

2.6 Conclusion

Of the 8 eligible papers found in the literature survey, 4 contain useful information for the programming gait motion in the Alpha 1 robot. The data from these group 1 papers consists of: shank pitch angular velocity data, shank to vertical angle during midstance of gait, foot and shank angular velocity, and 3-axis peak-to-peak velocity of the centre of mass. 3 papers contain angular data from the following analysis methods: MTS assessment, DAROM tests, and the PT. These group 2 papers can be used to program the movement of the Alpha 1 robot to mimic these specific tests. The final paper focuses on the range of movement in the arms of an individual with CP. The group 3 paper may be used alone to program the movement of the Alpha 1 robot's arms.

With the information gathered from the 8 eligible papers, it is possible to program motion into the Alpha 1 robot that mimics some traits of typical CP movement during gait, various clinical assessments and reaching tasks. However, the data available in the literature only provides a limited description of the overall movements, and so the movement of the Alpha 1 robot may only moderately reflect typical CP movement.

Chapter 3

Methodology

3.1 Introduction

A survey of the literature found 8 papers which present numerical data that could potentially be used for programming the Alpha 1 humanoid robot. [17] was chosen as a focus paper, as it presents a multitude of numerical data of both typically developed (TD) and CP people for a specific clinical test, the PT. The PT is a simple exercise when compared to a movement such as CP gait. It is a perfect starting point for programming human motion into the Alpha 1 robot, due to its simple nature and the ability to validate the likeness of programmed motion to the real human data from [17].

The PT is a commonly used clinical test to measure spasticity. It uses gravity to provoke the muscle stretch reflex during passive swinging of the lower leg [17]. An illustration of the PT is shown in figure 3.1. To track the motion of the shank during the PT, a custom-built WATD was used. The WATD design and function is laid out in [5]. The WATD tracks motion in 9-axis directions, as explained in section 2.1, but since we were only interested in the angular motion of the PT, only the gyroscope data was used in this study. The gyroscope captures angular velocity in 3-axis directions. By integrating this data with respect to time, the WATD can be used to measure the angle of the shank during the PT. We first developed a method for data collection from the WATD using the Alpha 1 robot and then used this method to collect data from healthy human participants who imitated CP motion during the pendulum test.

In this chapter, section 3.2 explains the experimental setup for the human and robot data collection trials, section 3.3 goes through the data processing and analysis techniques, and section 3.4 describes the movement activities performed by the Alpha 1 robot and healthy human research participants.

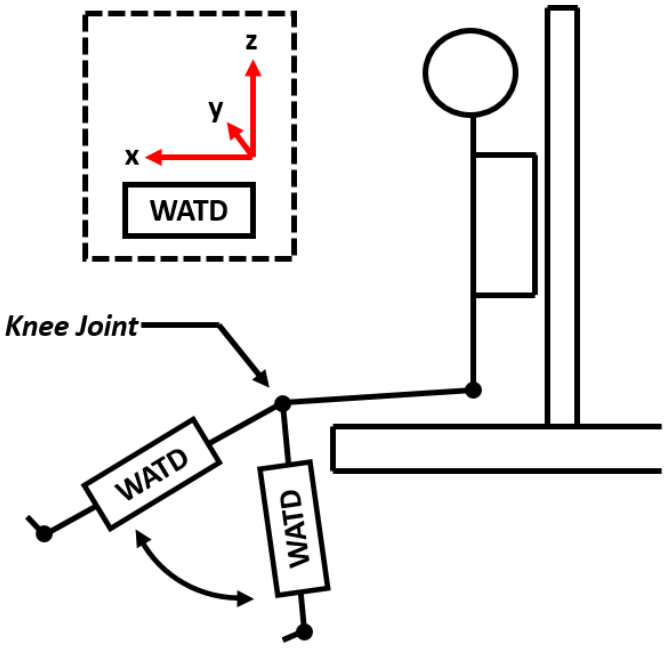

Figure 3.1: An illustration of the PT. Oscillatory shank motion is indicated by the arrow. The measurement axis directions of the WATD are shown in the dashed rectangle.

3.2 Experimental Setup

3.2.1 Apparatus for Equipment Setup

The experimental apparatus is shown in figure 3.2. Additionally, a computer and local Wi-Fi network are required to retrieve the data from the WATD.

Wearable Activity Tracking Device Specifications

The WATD is a small, custom-built device capable of tracking 9DOF motion data and sending this data over Wi-Fi to a nearby computer (an edge-computer). We used the WATD to acquire motion data from the Alpha 1 robot and human research participants. It can be seen in panel (d) of figure 3.2. The device had a width of 46mm, a length of 58mm, height of 47mm (including the battery and measuring the greatest dimension, as the WATD was not perfectly rectangular) and a weight of 81g (including battery). A 9V battery and 5V voltage regulator were used to power the WATD. The WATD consisted of two modules - the Wemos D1 Mini ESP8266 Wi-Fi module and the MPU9250 IMU. The MPU9250 was responsible for tracking the motion of the WATD in 9DOF,

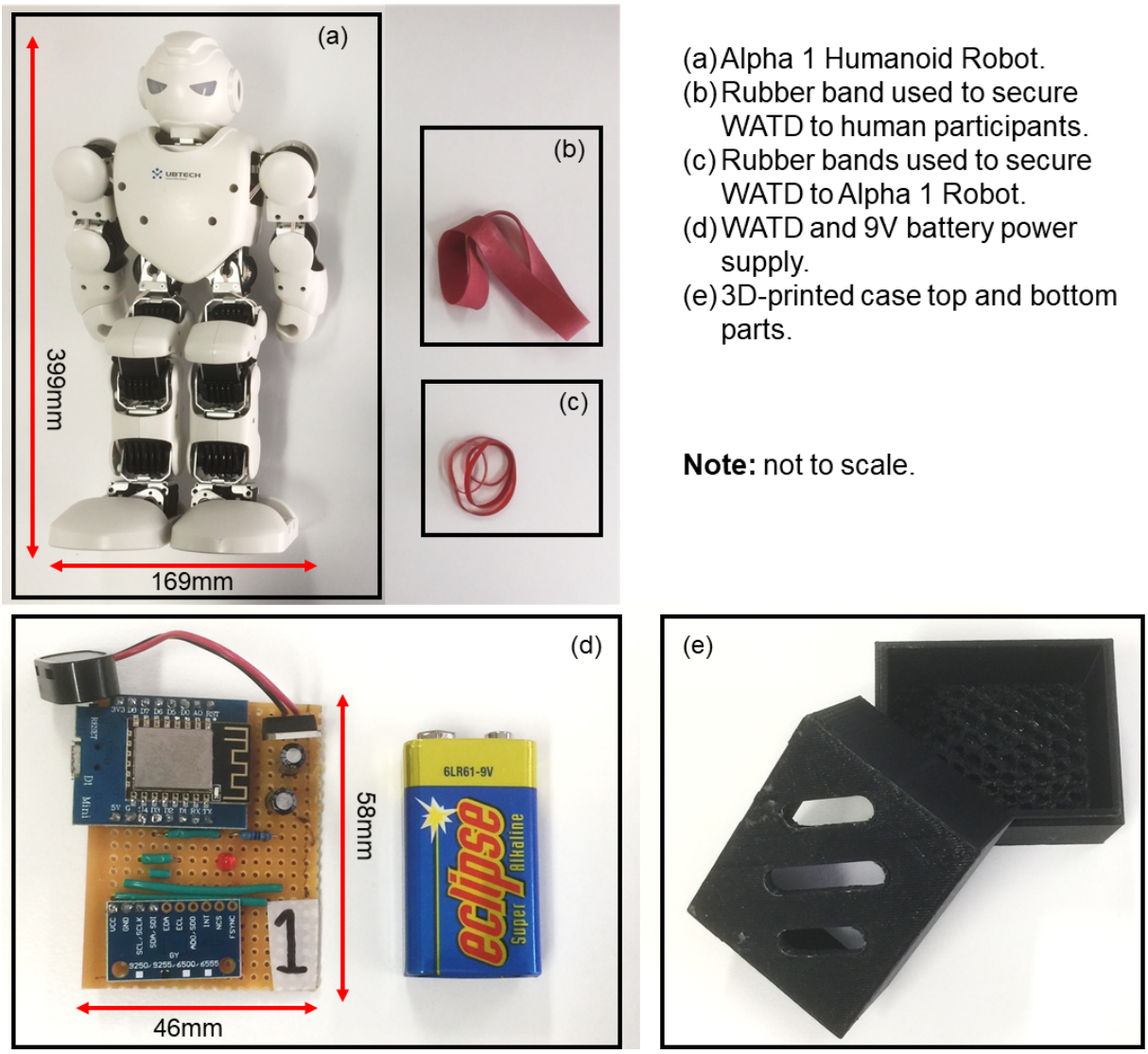

(a) Alpha 1 Humanoid Robot.
(b) Rubber band used to secure WATD to human participants.
(c) Rubber bands used to secure WATD to Alpha 1 Robot.
(d) WATD and 9V battery power supply.
(e) 3D-printed case top and bottom parts.

Note: not to scale.

Figure 3.2: The experimental apparatus used to gather motion data.

and this was shared with the Wemos D1 Mini's onboard microcontroller unit (MCU) via Inter-Integrated (I2C) communication. The MPU9250 was set to a full-scale range of 1000 degrees per second [5].

9DOF motion data was stored in the MCU memory of the Wemos D1 Mini. Data was accessed by the user over Wi-Fi through a server hosted on the ESP8266 Wi-Fi module in the Wemos D1 Mini. The server also provided control of the device, allowing the user to reset the WATD memory once it was full. The server was accessed by a PC or other device connected to the internet (locally or in another network). The WATD was able to store 1000 separate entries of 9DOF data. The tracking period could

be varied, to a maximum tracking frequency of 100Hz (10ms period). The maximum tracking time of the WATD until the memory reached capacity was directly dependent on the period that was specified for data collection. In this study, a 10ms period was used, so the maximum tracking runtime of the device was 10 seconds. The LED of the WATD was used to indicate WATD state information to the user, such as a successful connection to Wi-Fi, when motion data was being tracked, when the memory was full, and when the Wi-Fi server was accessed by a client [5].

3D-Printed Case Design

A custom case to house the WATD was designed and 3D-printed. Autodesk Inventor 2020 [29] was used to design the top and bottom parts of the case. The two parts of the case clip together with a simple mirrored step pattern along the connecting walls. The case has a width of 58mm, a length of 73mm, a height of 68mm, and a weight of 31g. There are several slits along the roof of the case which allow for the WATD LED to be seen when in use. To print the case, a FlashForge Dreamer 3D printer [30] was used. The 3D-printed case can be seen in panel (e) of figure 3.2.

3.2.2 Alpha 1 Humanoid Robot

To wirelessly collect 9-axis motion data from the Alpha 1 robot, the WATD was attached to the front of the Alpha 1's right shank with several small rubber bands. Data was collected with and without the use of the 3D-printed case. The Alpha 1 humanoid robot was perched on the edge of a desk and its torso was tightly secured to a weighted bookend with a latex band. This positioning allowed the right shank of the Alpha 1 to swing unencumbered while the robot remained secured in place. A photo of this setup with the 3D-printed case can be seen in figure 3.3. When the case was not used, the WATD was placed in a small bubble wrap pocket and fixed directly to the Alpha 1 robot's shank in the same position.

3.2.3 Human Data Collection

To wirelessly collect 9-axis motion data from human participants, the WATD was attached to the front of the right shank close to ankle with a large rubber band. The 3D-printed case was always used during human data collection. Figure 3.4 shows a participant wearing the WATD during the PT. A detailed description of the PT administered on the participants is given in 3.4.2.

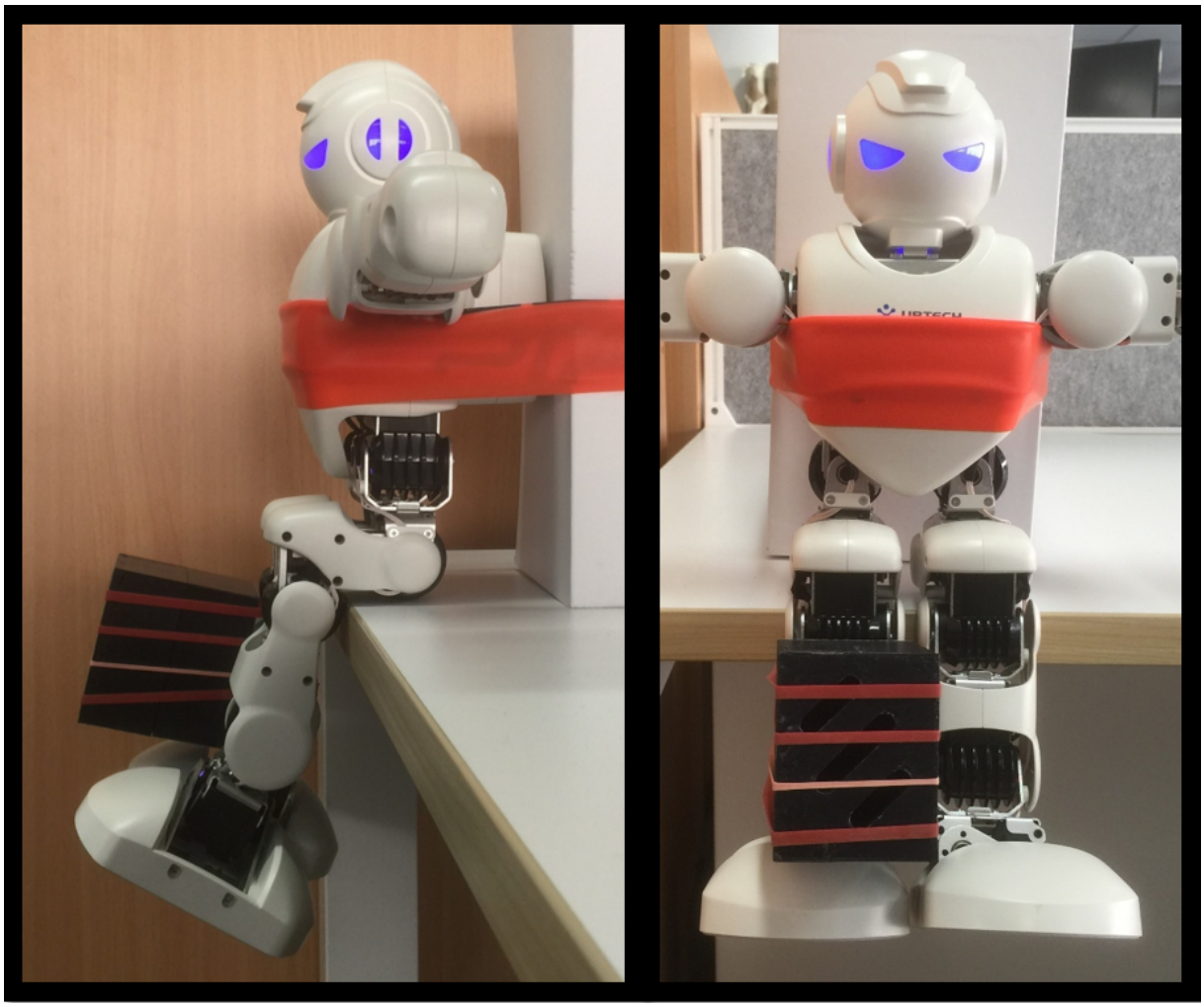

Figure 3.3: Side and front on views of the experimental setup of the Alpha 1 robot during shank movement data collection (with case).

Participants

A total of 7 (6 male and 1 female) research participants were included in this study. Participants fell within the height range of 155-190cm, had an age range of 23-27 years and an average age of 23.86 years, and were TD (no issue in physical movement due to disease, injury or other condition). None of the participants had undergone surgery during the year prior to the study. All research participants were recruited from the student population of Macquarie University.

Figure 3.4: Side and front on views of the human experimental setup and WATD placement during the PT. The WATD is secured to the right shank close to the ankle.

3.3 Data Processing and Analysis

The gyroscope of the WATD records 3-axis angular velocity measurements (in units of °/s) with a 10 millisecond period. To convert this data to angular displacement (in units of °), cumulative trapezoidal numerical integration of the data was performed in MATLAB [31]. However before integrating, the raw angular velocity data must be calibrated to ensure the angle calculated from the velocity measurements is accurate. The application of this principle is discussed in subsection 3.3.1. To further improve the accuracy of the WATD angle measurements for these specific movements, the vector of the angle data was taken. The reasoning and methodology behind this is discussed in subsection 3.3.2.

3.3.1 Device Calibration

The gyroscope requires calibration to eliminate errors in the raw data measurements. The gyroscope measures angular velocity in each axis direction. These measurements can be written in the form of equation 3.1, where ω is the x-, y- or z-axis angular velocity measurement recorded by the gyroscope, ω_a is the actual angular velocity in that axis direction, and ω_0 is the constant DC shift error in the gyroscope measurement.

$$\omega = \omega_a + \omega_0 \tag{3.1}$$

To calculate the angular displacement, the angular velocity is integrated by performing cumulative trapezoidal numerical integration of the data in MATLAB [31]. This principle is seen in equation 3.2, with θ representing the angular displacement, or how many degrees the WATD has travelled in that axis direction. The constant DC shift error in the gyroscope measurements, ω_0, becomes a linear term for the angular displacement, $\omega_0 t$. This causes linear drift in the angle calculation.

$$\theta = \int_0^t \omega \, dt = \omega_a t \; + \; \omega_0 t \tag{3.2}$$

To eliminate the drift in the angular displacement measurement, the constant DC shift error in equation 3.1 was estimated and subtracted from the angular velocity measurements. This was done by averaging a total of 27000 data points while the device was still, meaning angular velocity measurements should remain at 0°/s, and so any value measured by the gyroscope would be due to constant DC shift error and random fluctuation errors. 3000 data points were collected with 3 different orientations of the WATD for each axis, making a total of 9000 data points for each axis. The 3 orientations of the WATD were such that the x-y, x-z or y-z planes were parallel to the earth. The calculated error for each axis direction is subtracted from the raw gyroscope data for all other data collection activities.

3.3.2 Angular Measurements

During the PT, angular movement of the Alpha 1's shank is isolated around a single axis located at the knee. This is the y-axis in figure 3.1. Due to this, it is feasible to take the vector magnitude of the x-, y- and z-axis angular displacement measurements to obtain the total angular displacement of the shank. This compensates for misalign-

ments of the WATD on the shank, which cause a fraction of the y-axis direction angle measurements to be captured in the x- or z-axis direction, resulting in a lower angle measurement than expected. Equation 3.3 was used on the calculated x-, y- and z-axis angle data (θ_x, θ_y and θ_z respectively) to obtain the total angle vector of the exercise, θ_{total}.

$$\theta_{total} = \sqrt{\theta_x \times \theta_x + \theta_y \times \theta_y + \theta_z \times \theta_z} \tag{3.3}$$

To compare the total angular displacement vector with the values used to program the Alpha 1 robot, the total angular displacement vector was flipped and aligned with the programmed values. First the total angular displacement vector was flipped (multiplied by -1), then the starting angle value was added to the vector, and finally the first point of change was shifted to 0ms. This changes the total angular displacement vector to be in terms of the angle of the knee servo (servo ID9) used to program the alpha 1 robot.

After converting the measured angle data to be in terms of the Alpha 1 ID9 servo, the accuracy of measurements are judged through the use of graphs, resting angle (RA) values, and the root-mean-square error (RMSE) and cross-correlation (R) with the programmed angle.

For the human PT, the motion of the shank is not as perfectly aligned around the y-axis in figure 3.1 as it is with the Alpha 1 robot. During the pendulum oscillations of the human shank, there is some side-to-side movement due to the mobility of the hip joint allowing the upper leg to move and rotate. This side-to-side motion is much smaller than the oscillations of the shank around the knee joint however, and misalignments of the WATD on the shank have more effect on the angular measurement, so equation 3.3 was also used when processing human data.

3.4 Movement Activities

3.4.1 Repetitive Shank Oscillation

As the PT was selected as an exercise to focus on in this study, the accuracy of the WATD when tracking angular oscillations needed to be assessed. A repetitive shank oscillation exercise was programmed into the Alpha 1 robot for this purpose. During the repetitive shank oscillation exercise, the Alpha 1 robot was programmed such that

angle range and number of swings fell within the typical ranges of the PT (given later in table 3.2). 3 different oscillation frequencies were used. Parameters of the repetitive shank oscillation exercises can be seen in table 3.1. Note that the oscillation exercise nomenclature is such that the trial name is derived from the half-period of the shank swing.

Table 3.1: Parameters of the 3 repetitive shank oscillation exercises. Angles refer to the programmed angle of the Alpha 1 knee servo (servo ID9).

Trial Name	Half period (ms)	Extension Angle (°)	Flexion Angle (°)	Angle Range (°)
200ms Oscillation	200	140	80	60
500ms Oscillation	500	140	80	60
800ms Oscillation	800	140	80	60

During the repetitive shank oscillation trials, motion data was captured by the WATD as described in section 3.2.2.

3.4.2 Pendulum Test

The PT was administered on human participants and was mimicked by the Alpha 1 robot from data gathered in the literature. An illustration of the PT is shown in figure 3.1. This section describes how the PT activity was designed for the Alpha 1 robot and how it was administered on human participants.

Alpha 1 Robot Activity Design

To imitate human movement during the PT, the Alpha 1 humanoid robot was programmed from real human movement data captured from the shank during the PT. This data is available in the literature, specifically taken from [17]. 4 metrics from results data of the right leg of the reference (Ref) group and right leg of the spastic diplegia (SD) group in [17] were used. Herein, the Ref group metrics have been used to characterize the movement of a TD person, and the SD group metrics have been used to characterize the movement of a person with CP. The TD and CP metric descriptions and values are shown in table 3.2.

The metrics in table 3.2 were used to produce a waveform model for the TD and CP groups which outputs values that are used to program the Alpha 1 humanoid robot's right knee servo (servo ID9). Assuming a RA for servo ID9 of 70° means at rest the shank is roughly perpendicular to the ground as a human shank would be. From

Table 3.2: PT metric descriptions and values for TD and CP volunteers. This data is not my own, but borrowed from [17] to program the Alpha 1 robot.

Metric	Description	TD	CP
EX (°)	The first swing excursion. The difference between the starting angle and the first angle of reversal swing.	95	55
RI	The relaxation index. Calculated as follows: (starting angle - first angle)/(starting angle – resting angle). The resting angle (RA) is the angle measured at the knee joint when the shank has stopped oscillating.	1.2	0.85
T (s)	The duration of oscillations. The time from the start of the PT until the shank comes to rest.	5.6	2.1
n	The number of shank oscillations before coming to rest.	7	4

the RA, the other angles were calculated using the RI in table 3.2. The model only provides peaks, troughs and an endpoint, which gives a triangle waveform output. It is assumed for simplicity that each wave has an equal period and that the peak and trough amplitudes decrease linearly towards the RA.

Initially, the PT was performed by the Alpha 1 robot to monitor how accurately the WATD could track the motion. Following the human trials, a direct comparison of trial variability for Alpha 1 versus real humans was needed. To achieve this, data was collected for 60 trials each for the TD and CP PT motions, reflecting the total number of human trial datasets used in the study.

During the Alpha 1 robot's PT trials, motion data was captured by the WATD as described in section 3.2.2.

Human Trials

The procedure for the PT administered on human research participants was performed as described in [17]. Research participants were seated on a desk which was of adequate height to allow for uninhibited swinging of the shank. Participants were instructed to recline approximately 20° from the vertical to reduce any possible effects of hamstring tightness. Each participant sat with their knees far enough away from the edge of the desk to avoid their shank contacting with the desk at maximum knee flexion. Figure 3.4 shows a research participant in this position.

Each participant performed 2 sets of 10 PT trials. The first set was the true PT, measuring the participants' natural response to passive movement. This is referred to as

the TD category in the results. The participant was instructed to remain relaxed and refrain from actively controlling any of their leg muscles during this PT. Participants were asked to repeat a TD PT trial if the tester noticed any active control of the shank through observation. The second set of PT trials was the CP category, where participants were asked to mimic the motion of a person with CP during the PT by actively tensing their quadriceps muscles. Participants were instructed to close their eyes to prevent them from influencing how their shank oscillated based on visual feedback. After each of the TD and CP trials, the participant was given a minimum of 30 seconds rest to ensure their muscles did not become fatigued. Participants were given a chance to familiarise themselves with these motions before their motion data was recorded.

For the TD PT trials, from the participant's seated and relaxed position on the edge of the desk, the tester raised the right shank of the participant to maximum extension. The WATD was switched to the data tracking mode, and the leg was held in place for around 1 second to ensure the entire PT motion was captured. The shank was dropped by the tester and left to passively pendulum until it came to a complete rest. The tester saved the data captured by the WATD and allowed the participant time to rest before repeating for a total of 10 trials.

For the CP PT trials, from the participant's seated and relaxed position on the edge of the desk, the tester again raised the right shank of the participant to maximum extension. The WATD was switched to the data tracking mode, and the leg was held in place for around 1 second to ensure the entire PT motion was captured. The shank was dropped by the tester and swung with a truncated pendulum motion due to active muscle control by the participant before coming to a complete rest. The tester saved the data captured by the WATD and allowed the participant time to rest before repeating for a total of 10 trials.

During the human PT trials, motion data was captured by the WATD as described in section 3.2.3. The 4 metrics mentioned in table 3.2 were extracted from the human data sets and used in the comparison and analysis of the PT results.

Chapter 4

Results and Discussion

4.1 Device Calibration

The error calculated for each of the still trial orientations and the average error for each axis is shown in table 4.1. Each axis error remains consistent independent of the orientation of the device. It is therefore likely that the WATD will always record gyroscope data with an offset close to these values regardless of WATD orientation during physical activity when it is still. The error values may deviate when the device is in motion, but this is harder to test as there are multiple variables.

Table 4.1: The error recorded for each gyroscope axis during the 3 still trials and the average error amongst the trials.

	x-axis Error (°/s)	**y-axis Error (°/s)**	**z-axis Error (°/s)**
x-y plane parallel to earth	-0.0880	-0.7560	-1.2402
x-z plane parallel to earth	-0.0821	-0.7419	-1.2545
y-z plane parallel to earth	-0.0968	-0.7629	-1.2515
Average DC shift error	-0.0890	-0.7536	-1.2487

Figure 4.1 shows the recorded raw 3-axis gyroscope data for a single still trial of the WATD in panels (a), (c), and (e). By subtracting the average error from each axis recording, these data sets are centred around the 0°/s line and have a new average value of 0°/s, as is expected when the WATD is not in motion.

The effect of calibrating the raw gyroscope data can be seen in figure 4.1 panels (b), (d), and (f). As the WATD is not moving during the still trial, no angular displacement is expected in any axis direction. The calculated angle from the data that has not been calibrated (full lines in figure 4.1 (b), (d), and (f)) shows a finite angular displacement

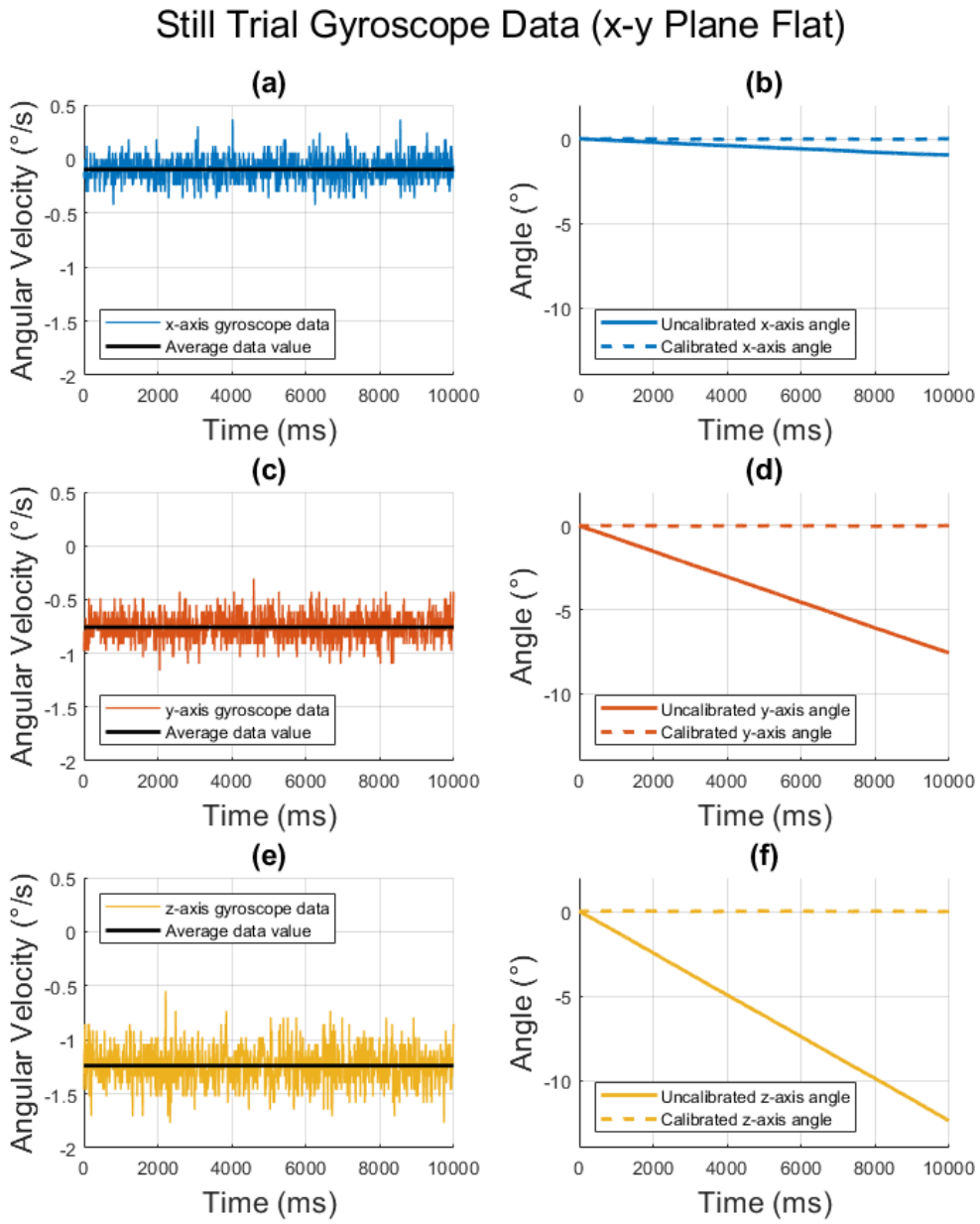

Figure 4.1: 3-axis angular velocity and angle data recorded by the WATD gyroscope during a still trial with x-y plane parallel to the earth. (a) raw x-axis gyroscope angular velocity data; (b) x-axis angle measurement with and without calibration of the raw data; (c) raw y-axis gyroscope angular velocity data; (d) y-axis angle measurement with and without calibration of the raw data; (e) raw z-axis gyroscope angular velocity data; (f) z-axis angle measurement with and without calibration of the raw data.

due to the error, $\omega_0 t$, in equation 3.2. By calibrating the raw gyroscope data before integration, this linear shift is effectively compensated for. This can be seen in the calibrated angle measurements (dashed lines in figure 4.1 (b), (d), and (f)), which remain very close to 0° for the entire trial.

The effect of calibration on the raw data sets can also be seen in figures 4.2 and 4.3. These figures are discussed further in their relevant sections (4.3 and 4.4.1). Calibration of the raw gyroscope data greatly improves the accuracy of the WATD angular measurements.

4.2 Effect of Case

The required height for the 3D-printed case was overestimated during manufacturing, meaning the empty space inside the case needed to be filled with padding (bubble wrap) to secure the WATD in place. The WATD LED had to remain visible to the tester during trials, so the WATD was positioned at the roof of the case near the slits and padding was placed below this. This caused the device to be approximately 25-35mm away from the surface of the robot or human shank during movement trials when the case was used. This distance between the case and shank has reduced the accuracy of recorded angle results. The oversized nature of the case may also allow the WATD to move around inside the case if the padding is not adequately thick, again reducing accuracy of WATD results. Instances of this occurring are laid out in sections 4.3 and 4.4.1.

The case was necessary in all human trials, as when fixing the WATD to humans the rubber band in 3.2 (b) exerts a significant amount of force which may have caused the uncovered WATD components to break off from the board. The effect of the case on human motion tracking has not been observed for this reason, but it is assumed that using the case will reduce the accuracy of recorded results as was seen with the Alpha 1 robot.

By reducing the size of the WATD itself and ensuring a secure fit inside the case, the distance between the WATD and the shank can be minimised and the WATD would not move around inside the case. Achieving this minimal distance and fixed orientation inside the case would allow the WATD to track results as accurately as seen in the ”without case” robot results in sections 4.3 and 4.4.1.

4.3 Repetitive Shank Oscillation

The WATD is able to track the motion pattern of the 3 repetitive shank oscillation exercises well. This can be noticed in figure 4.2 and is evident from the high cross-correlation values of the WATD measured angle with the programmed Alpha 1 angle seen in table 4.2 for all trials (>97.89%). Overall, calibration of the results is seen to improve the accuracy of the WATD, and use of the case when tracking is seen to slightly decrease the accuracy of recorded repetitive shank oscillation results.

Table 4.2: Root-mean-square error, resting angle measurement, and cross-correlation for the various repetitive shank oscillation trial data sets as compared with the Alpha 1 servo ID9 programmed angle. Note the resting angle for all trials should be 80°.

Trial	Calibration (Y/N)	Case (Y/N)	RMSE (°)	Resting Angle (°)	R
200ms oscillation	Y	Y	5.1897	86.2406	0.9875
		N	4.1120	80.8205	0.9925
	N	Y	6.0849	88.1170	0.9874
		N	3.9885	83.5674	0.9936
500ms oscillation	Y	Y	5.2599	85.1226	0.9945
		N	0.5260	80.3804	0.9997
	N	Y	6.8920	88.4801	0.9918
		N	3.0084	85.0258	0.9979
800ms oscillation	Y	Y	5.0250	85.8292	0.9934
		N	0.8191	81.0444	0.9994
	N	Y	7.2613	90.9075	0.9789
		N	3.7359	86.8095	0.9930

A feature noticeable in all trials is the smooth peaks and troughs of the recorded angle data waveforms seen in figure 4.2. The Alpha 1 is programmed to follow the sharp-peaked, triangular waveform, but the recorded angle data always shows smooth peaks and troughs. This may be an inadequacy of the WATD, or the Alpha 1 robot servomotor may not be able to change directions fast enough to replicate these sharp peaks.

The Alpha 1 robot has some limitations on how fast its servomotors can move. This is seen in the 200ms repetitive shank oscillation trials (panels (a) and (b) of figure 4.2). Referring just to the calibrated data recorded without the case, the measured angle waveforms show a reduced amplitude when compared to the programmed angle, more so than is seen in the 500ms and 800ms trials. This could be an inaccuracy of the WATD, but it is likely a limitation of the Alpha 1, as a reduced amplitude of this degree is only recorded in the 200ms trial. Also visible is the small overshoot of the recorded

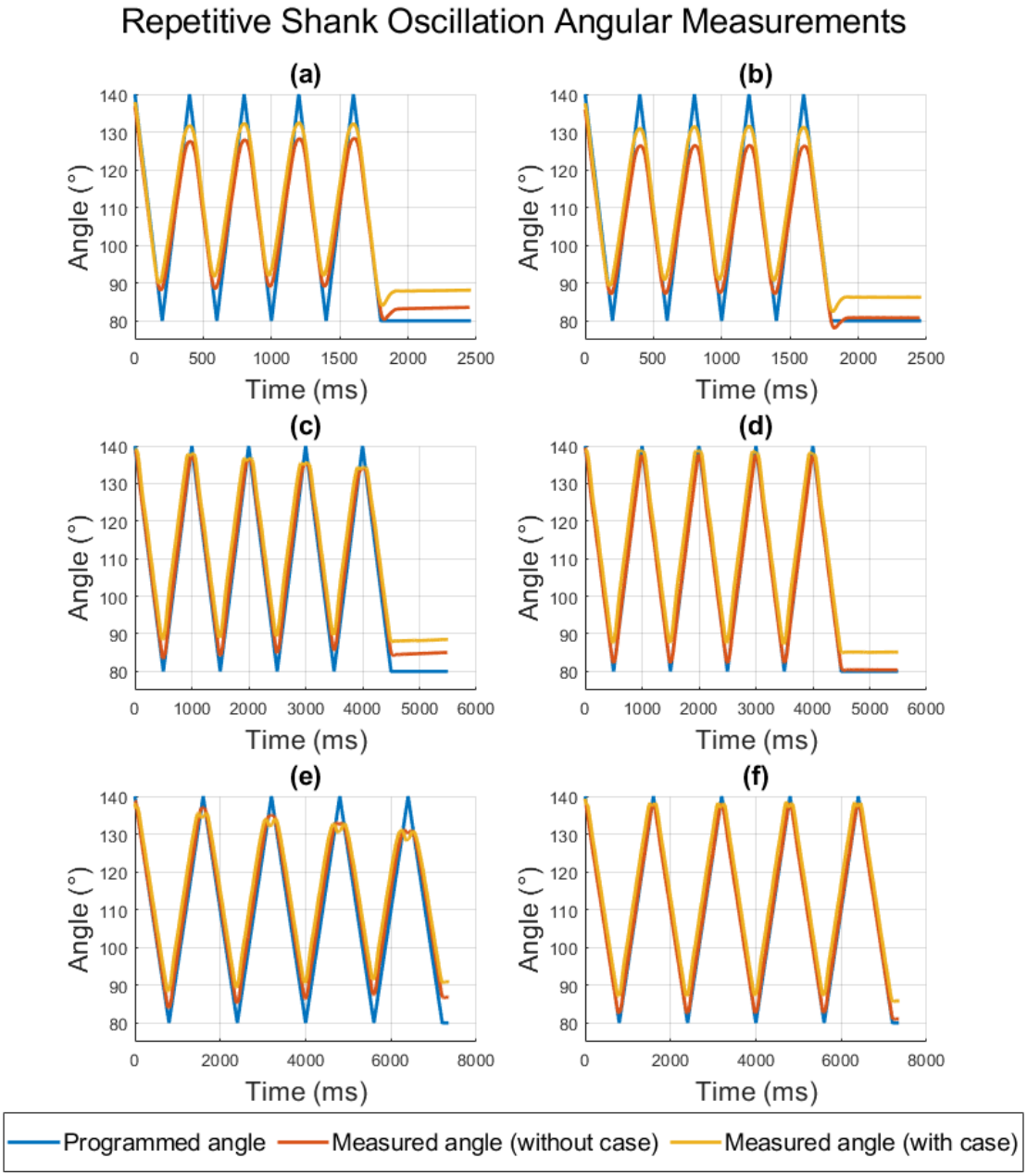

Figure 4.2: Angle measurements recorded during the various repetitive shank oscillation trials. (a) 200ms oscillation trial angle measurements without data calibration; (b) 200ms oscillation trial angle measurements with data calibration; (c) 500ms oscillation trial angle measurements without data calibration; (d) 500ms oscillation trial angle measurements with data calibration; (e) 800ms oscillation trial angle measurements without data calibration; (f) 800ms oscillation trial angle measurements with data calibration.

data just before it reaches the RA. Similarly, this is only seen in the 200ms, so is likely an error of the Alpha 1 servomotor when moving at this speed.

The calibration performed on the data described in section 3.3.1 improves the accuracy of the WATD in the repetitive shank oscillation trials. Visually, this is seen in figure 4.2 with the closer match of the data to the programmed angle when calibration is used. It is most visible at the peaks, troughs and especially comparing the differences in measured RA. In the 500ms and 800ms trials, gyroscope drift causes increasingly drastic peak amplitude suppression as the trial progresses. Calibration of the raw data is shown to eliminate this almost completely. Table 4.2 shows calibration always brings the RA closer to the desired value of 80°, and is seen to reduce the RMSE by an average value of 2.033° among the trials (except in the 200ms oscillation without case trial where RMSE was seen to increase by 0.1235°).

In all of the repetitive shank oscillation trials, the case is shown to reduce the accuracy of the WATD. This is due to the reasons discussed previously in section 4.2. The RMSE and RA of the trials listed in table 4.2 are always worse when the case was used during data collection. Referring to the calibrated 500ms and 800ms trial data in figure 4.2 (d) and (f), the peaks are registered less accurately with the case - a flat line can be seen instead of a curved sinusoidal peak when the case is used. This is likely due to the WATD moving around inside the case as the shank abruptly changes direction at the top of the swing. It is much less noticeable on the bottom of the swing (a smooth sinusoidal curve is seen), which is probably due to the placement of the case padding below the WATD, which supported it during this direction change.

4.4 Pendulum Test

4.4.1 Alpha 1 Robot Results

Preliminary Trials

As with the repetitive shank oscillation trials, the WATD is able to track the motion patterns of the TD and CP programmed PT trials well. This can be noticed in figure 4.3 and is evident from the high cross-correlation values of the WATD measured angle with the programmed Alpha 1 angle seen in table 4.3 for all trials (>99.43%). As with the repetitive shank oscillation trials, calibration of the data is seen to improve the accuracy of the WATD, and use of the case when tracking is seen to decrease the accuracy of recorded PT results.

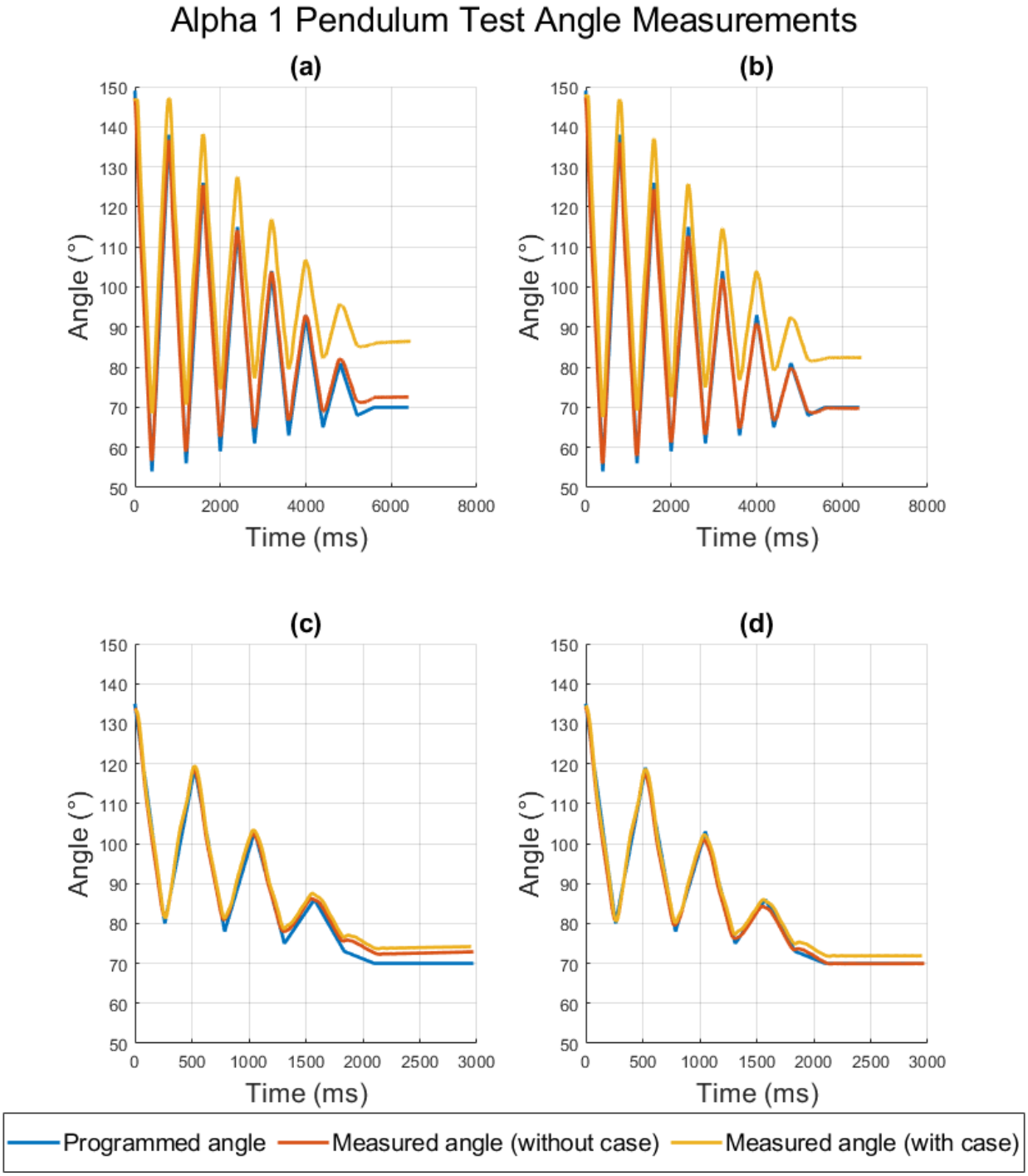

Figure 4.3: Angle measurements recorded during the Alpha 1 PT trials. (a) TD trial without data calibration; (b) TD trial with data calibration; (c) CP trial without data calibration; (d) CP trial with data calibration.

Table 4.3: Root-mean-square error, resting angle measurements, and cross-correlation for the PT trial data as compared with the Alpha 1 servo ID9 programmed angle. Note the resting angle for PT trials should be 70°.

Trial	Calibration (Y/N)	Case (Y/N)	RMSE (°)	Resting Angle (°)	R
TD	Y	Y	12.5306	82.3796	0.9966
		N	1.5585	69.7084	0.9964
	N	Y	14.9731	86.4499	0.9943
		N	2.4351	72.5657	0.9956
CP	Y	Y	1.6090	71.9205	0.9980
		N	1.1887	69.9592	0.9974
	N	Y	3.0328	74.2182	0.9972
		N	2.1019	72.9082	0.9966

The calibration performed on the data described in section 3.3.1 is shown improve the accuracy of the WATD in all PT trials. Visually, this can be noticed in figure 4.3 with the closer match of the data to the programmed angle when calibration is used. Again, it is most visible at the peaks, troughs and especially comparing the differences in RA. Table 4.3 shows that calibration of the raw gyroscope data always improves the measured RA and reduces the RMSE for both the TD and CP PT.

Similarly to the previous section, the case is shown to reduce the accuracy of the WATD in both PT trials. The RMSE and RA of the trials listed in table 4.3 are always worse when the case was used during data collection. In figure 4.3 panels (a) and (b), the effect of the case is more dramatic than in any of the repetitive shank oscillation results or the CP PT results. This may be because the shank is swinging with a higher amplitude in the beginning than in any of the other movements. However, without the case, the motion is recorded quite accurately.

These preliminary results are significant as they indicate the level of accuracy the WATD is able to achieve in recording angular results of movements in a single plane such as the PT. With further miniaturisation and development, this inexpensive WATD could be made even more accurate. Additionally, although the PT modelled from the literature is a somewhat simplified version of the real motion, these results show that the Alpha 1 can be programmed to follow a specific movement pattern. This verifies the ability of the Alpha 1 humanoid robot to act as a model for human movement.

Trials for Direct Comparison with Human Data

This section looks at the 120 (60 TD, 60 CP) PT trials recorded to match the amount of human data processed in the study. To copy the human results format and analysis (section 4.4.2), the data has been broken up into sets of 10 TD and CP trials, which are labelled as ”participants” 1-6 (p1-p6). In reality, data was all recorded from a single Alpha 1 humanoid robot. The average value of the 4 PT metrics (described in table 3.2) across the 10 trials for each of the participants has been extracted. These results are shown in figures 4.4, 4.5, 4.6 and 4.7 for metrics EX, RI, T, and n respectively.

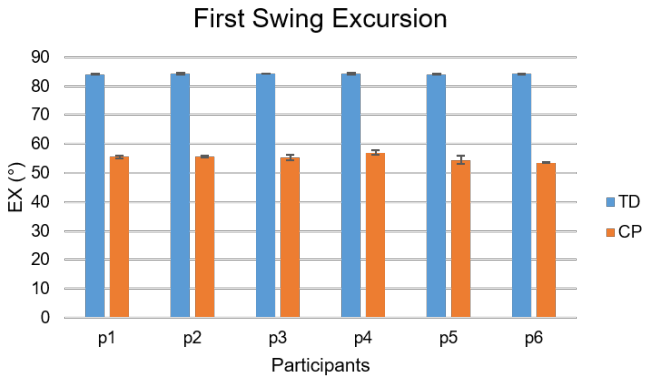

Figure 4.4: TD and CP EX means from the 10 trials with standard deviation error bars for the 6 robot participants.

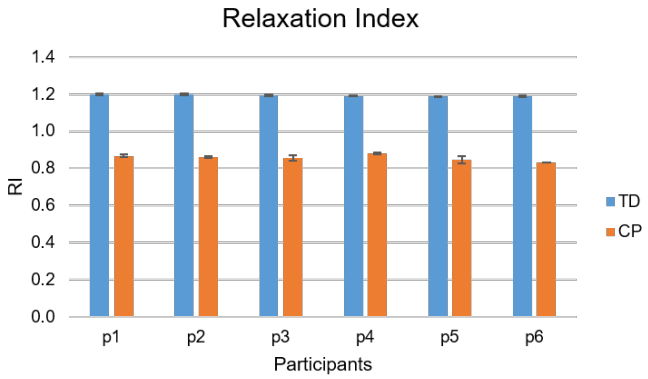

Figure 4.5: TD and CP RI means from the 10 trials with standard deviation error bars for the 6 robot participants.

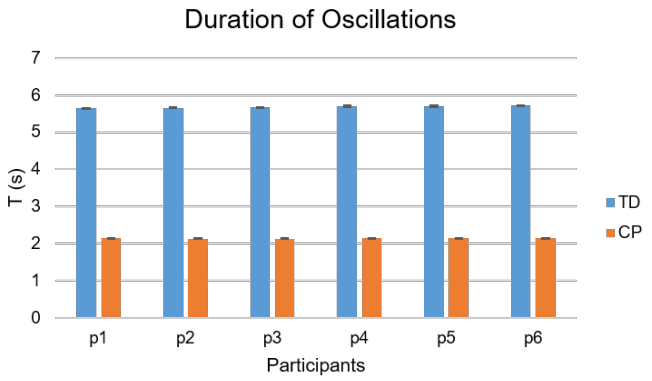

Figure 4.6: TD and CP T means from the 10 trials with standard deviation error bars for the 6 robot participants.

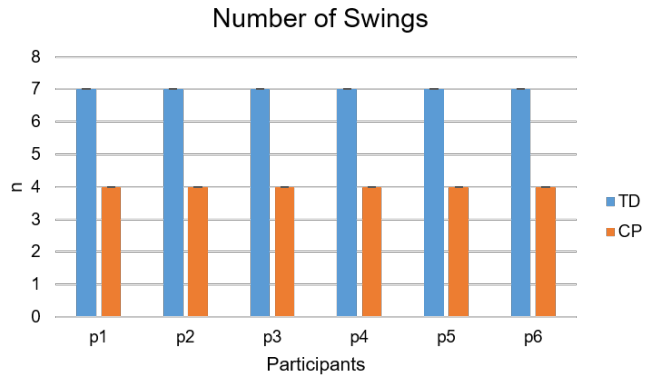

Figure 4.7: TD and CP n means from the 10 trials with standard deviation error bars for the 6 robot participants.

The values for the 4 metrics are extremely consistent over all the trials, shown by having similar means across participants and low standard deviation error bars. The average extracted metric values across all 60 TD or CP trials are close in value to the metric values used to develop both of the PT movement models. This is shown in table 4.4, with the measured TD EX value being the only metric which varies significantly between programmed and measured value. This was also seen in the preliminary results, referring to figure 4.3 panel (b). Optimization of the case as discussed in 4.2 would improve this result, as is shown by the measured angle when no case was used during the TD PT preliminary trial.

Table 4.4: Comparison of the programmed versus average extracted metric values for the 120 robot PT trials. The average was taken across all the TD or CP robot trials as a whole.

	TD		**CP**	
Metric	**Programmed**	**Measured**	**Programmed**	**Measured**
EX (°)	95	84.1812	55	55.2537
RI	1.2	1.1925	0.85	0.8567
T (s)	5.6	5.6805	2.1	2.1415
n	7	7	4	4

Although it was known that recording robot PT trials without the 3D-printed case measured more accurate results, the case was used in all 120 of these PT trials. This was to match the human data collection method, where the case was always necessary as discussed in section 4.2.

4.4.2 Human Results

1 of the 7 participants' data was discarded. This was due to the participant's shank swinging for longer than the tracking window of the WATD. The WATD tracking window was set to 10 seconds, which was done to optimise the sampling frequency for the expected duration of the average PT. However, this participant's shank swung for more that 10 seconds in most trials, so the end of the PT movement was not captured by the WATD. The PT test trials were recorded and analysed for the remaining 6 participants (5 male, 1 female).

An example of the angle data recorded during a single trial of both the TD and CP PT is shown in figure 4.8. Graphs such as these were generated for all of the individual PT trials, and from the total angle vector the 4 metrics were extracted and recorded. These figures look different from the previously presented Alpha 1 robot figures as the data is not put in the reference frame of the Alpha 1 knee servo. Instead, 0° represents maximum knee extension in these graphs.

The average value of the 4 PT metrics (described in table 3.2) across the 10 TD and CP PT trials for each of the human participants was extracted. These results are shown in figures 4.9, 4.10, 4.11 and 4.12 for metrics EX, RI, T, and n respectively. Participants 1-6 are labelled as p1-p6.

All participants show a higher average metric value in the TD trials, except for the RI value of participant 2, where a higher average was obtained in the CP trials. There

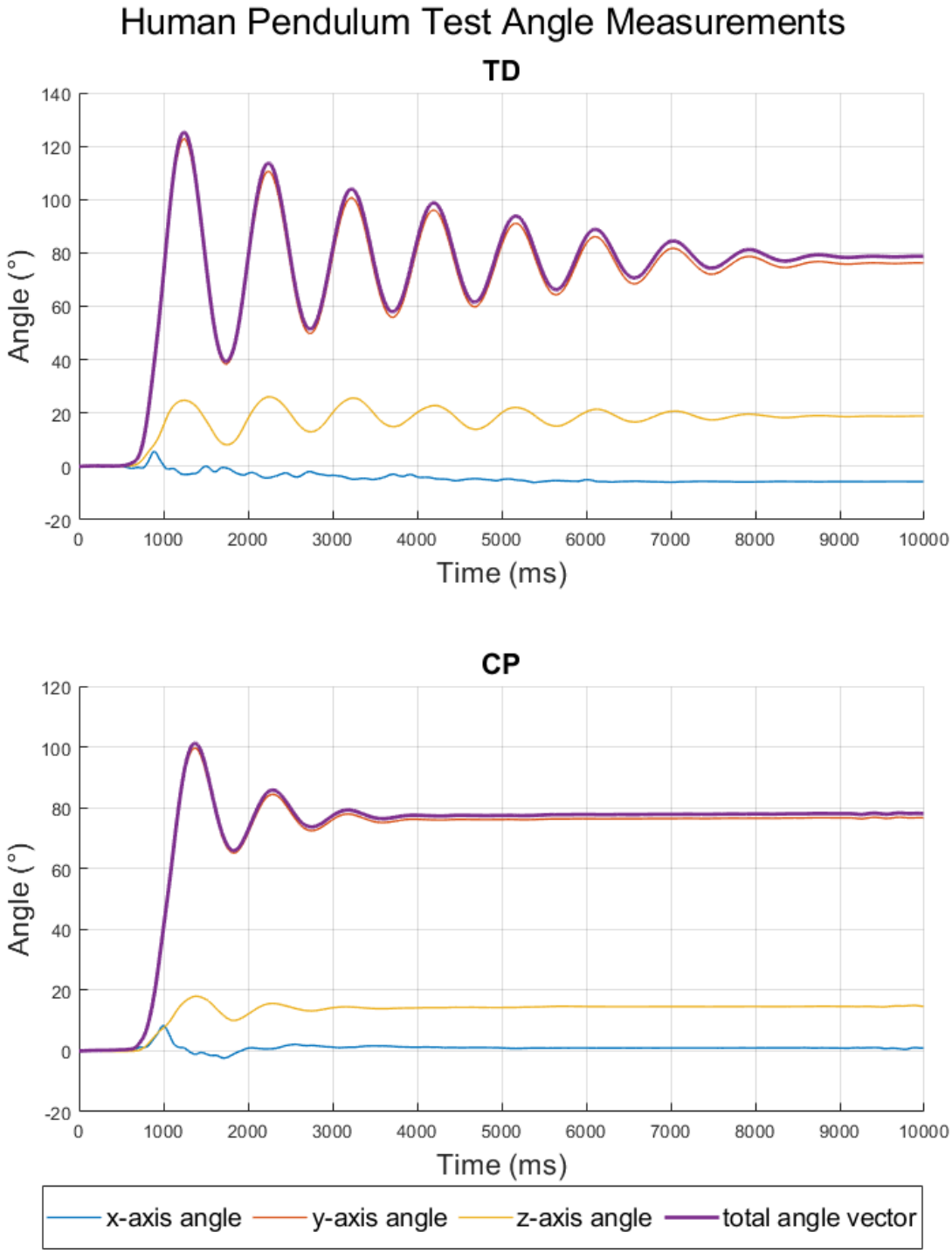

Figure 4.8: Angle measurements recorded during the human PT trials. Both the TD and CP graphs are a single trial taken from participant 6.

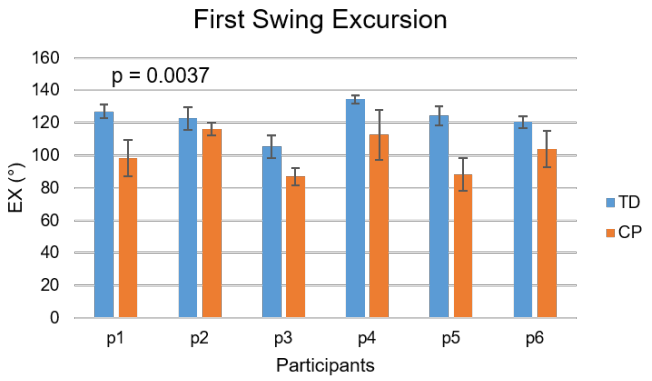

Figure 4.9: TD and CP EX means across 10 trials with standard deviation error bars for the 6 human participants.

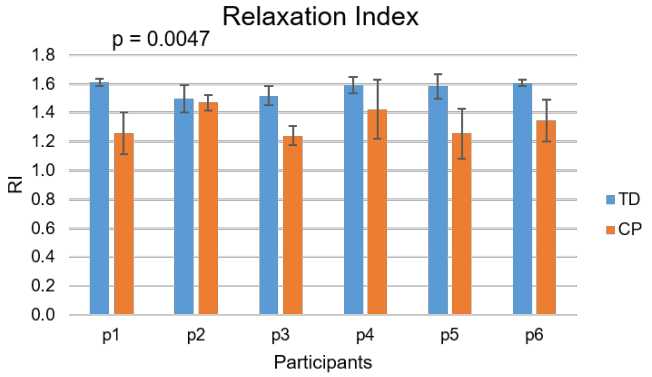

Figure 4.10: TD and CP RI means across 10 trials with standard deviation error bars for the 6 human participants.

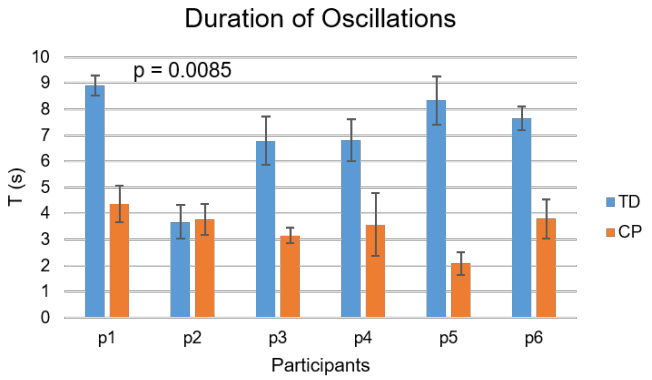

Figure 4.11: TD and CP T means across 10 trials with standard deviation error bars for the 6 human participants.

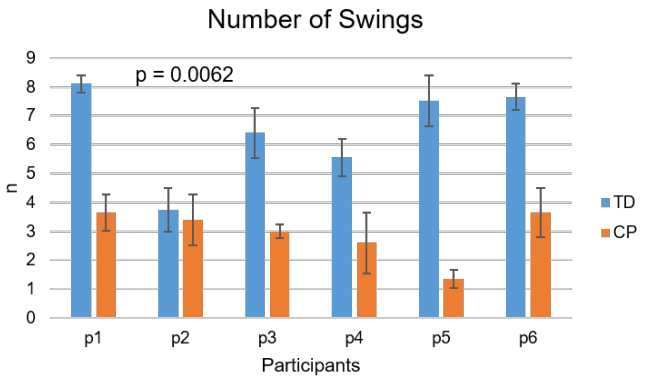

Figure 4.12: TD and CP *n* means across 10 trials with standard deviation error bars for the 6 human participants.

is a lot of variation in average metric values between the participants, except in the TD RI values, which are approximately 1.6 for 4 of the participants.

It is visible in figures 4.9-4.12 that the participants are generally able to achieve different results in the TD and CP PT when given instructions as laid out in section 3.4.2. Participant 2 is the only participant which shows similar average metrics between the two sets of PT trials. The low t-test p-values displayed on the graphs confirm the metric values are consistently different between the TD and CP PT. However, it is difficult to determine if this difference reflects an accurate representation of the PT performed on a person with CP.

As well as variation between participants, there is some individual variation between trials for each participant. This is seen in the standard deviation error bars in figures 4.9-4.12. Comparing the participants' individual average TD and CP metric values, 15 out of 24 show higher standard deviation in their CP trials. This means that the participants as a whole exhibit somewhat less similarity between CP trials than TD trials.

The measured average metric values for the 6 participants differ from the metric values found in the literature (listed in table 3.2). However, the results borrowed from the literature are from children. In [17], the TD group had an average age of 8 years and the SD group 10.33 years, whereas the participants in this study had an average age of 23.86 years (24 years not including the participant whose data was discarded).

A population of 7 is small for this type of study. A population in the order of 10-100 people would be more significant. A wider age range of participants would also provide more significant results. The 1 year time frame (with effectively 10 months of research work) of the Macquarie University Master of Research qualification and the

ethical approval process made it difficult to have a population of such a significant size. The participant age range was narrow as participants were recruited from the Macquarie University student population, which favours recruitment of young adults. To improve the validity of this study, it is planned to acquire data from a larger population with a wider age range in the future.

4.4.3 Justification for Using the Pendulum Test

In clinical application, the PT is used as an objective measurement of spasticity [17]. Development of such measurement methods has been researched thoroughly since the introduction of "spasticity management" [32]. These scales are used extensively in clinic as they do not require complicated equipment and are non-invasive, uncomplicated techniques [16, 17]. Other examples of such scales are the MTS, MAS and the DAROM tests - all of which appeared in the literature review (chapter 2). The various scales and tests all require a tester to either move or drop a limb to induce passive motion, perhaps at varying speeds.

The most useful and extensive data in the literature regarding CP movement tracked with wearables was data from the PT. This is why the PT was chosen as a focus exercise in this study for programming CP human movement into the Alpha 1 robot. However, as the clinical scales and tests are quite similar in their fundamentals, the development of the WATD and Alpha 1 human movement model in this study could easily be translated to modelling these other scales and tests.

4.5 Humanoid Robots as a Model for Clinical Movement

Humanoid robots have several advantages over using human participants for CP motion imitation. The movement of robots can be controlled exactly, whereas humans will always have some error in their movements. One can also compare measured data to programmed data with robots, which is not applicable for humans. As seen when comparing the various graphs in sections 4.4.1 and 4.4.2, human participants showed much more variation than the Alpha 1 robot when performing the PT. This is explicitly shown for all metrics in figures 4.13-4.16. The Alpha 1 robot can repeat PT trials much more accurately than the human participants.

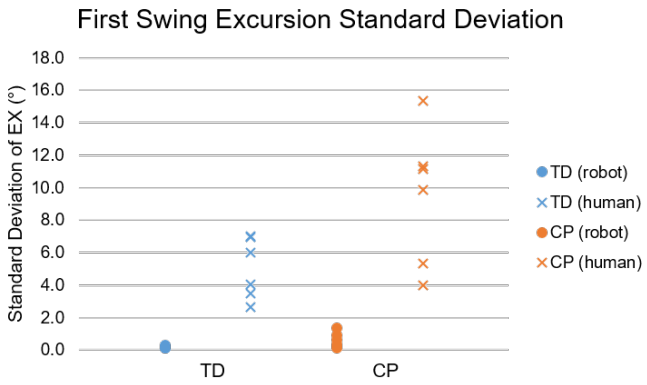

Figure 4.13: A scatter plot of all human and robot participants' EX standard deviation across the 10 TD and 10 CP PT trials.

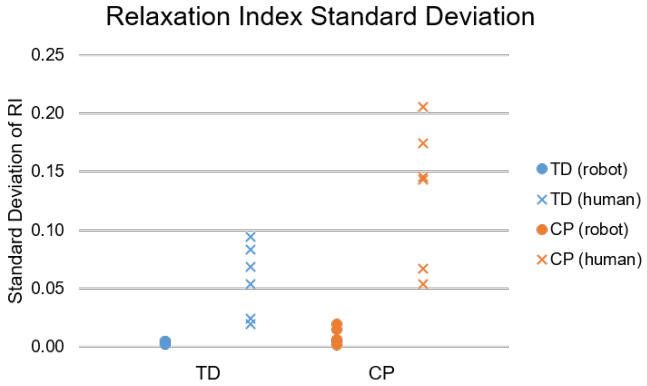

Figure 4.14: A scatter plot of all human and robot participants' RI standard deviation across the 10 TD and 10 CP PT trials.

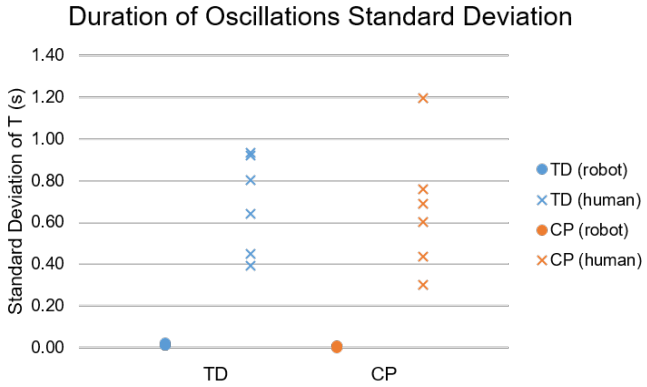

Figure 4.15: A scatter plot of all human and robot participants' T standard deviation across the 10 TD and 10 CP PT trials.

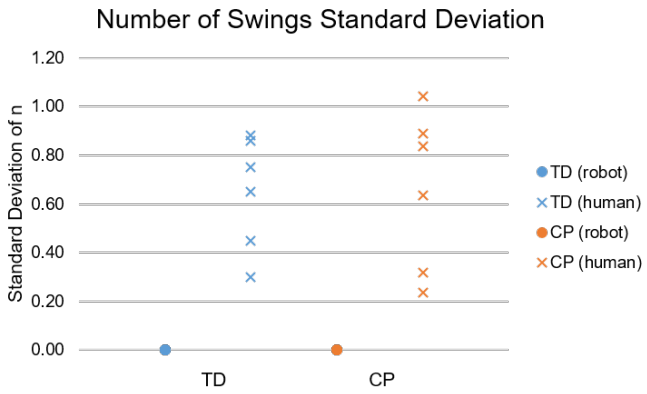

Figure 4.16: A scatter plot of all human and robot participants' *n* standard deviation across the 10 TD and 10 CP PT trials.

It is also easier to acquire data from humanoid robots than it is from humans. Ethical approvals to allow research with human participants take time to obtain, but these are not necessary when using robots. Access is also limited when studying a population like people with CP, through lengthy ethical approval processes and the small general population of such people. A large human population is necessary for study results to be significant, whereas a single robot can be programmed to move with as many variations as required to simulate a large population sample. It also takes more time to record data from a human participant than a robot, with equipment setup for each new person and participant recruiting and briefing. Human error (tester or participant) can also be minimised or eliminated from research trials with the use of robots.

In the future, we plan to record our own PT data from people with CP and program the Alpha 1 robot with this data. However, this was not the scope of the current project, having an effective research time frame of 10 months during the Macquarie University Master of Research qualification. As the Alpha 1 robot was programmed using human PT data from the literature, we did not directly correlate our research participant PT data with the Alpha 1 PT data. Future work of programming the robot with our own data will allow us to perform a statistical analysis to find a direct correlation between the two data sets and improve the accuracy of the Alpha 1 robot's imitation.

There are drawbacks to using humanoid robots in research. The robot is only a model, and as such its imitation of human movement will not be identical to real human movement. Humanoid robots are only useful in specific applications. Humanoid robots are often also at a smaller scale to real humans, especially in our case where budget was a limiting factor.

4.6 Evaluation of the Wearable Activity Tracking Device

There are commercially available solutions for wireless motion tracking, such as the various IMUs from Xsens [1] and the Blue Trident IMU from Vicon [2]. These IMU systems cost upwards of 10-20 times the amount spent on the WATD components. It was not feasible to purchase a commercial wireless tracking IMU with the Master of Research budget. Future work by other researchers can focus specifically on comparing the results from our WATD device with the commercial IMUs. However, it is worth mentioning that these commercially available devices are not compatible with the edge-computing architecture described in [5] and [6], which was specifically the case with our WATD.

Chapter 5

Conclusions and Future Work

5.1 Conclusions

This study aimed to validate a previously developed custom-built WATD and gauge the suitability of the Alpha 1 humanoid robot as model for human movement in clinical CP research. Leveraging off the programmability of the Alpha 1, the WATD was shown to track angular data from various oscillatory motion patterns accurately and with low variability. PT data from the literature was used to program the Alpha 1 robot, allowing it to act as a model for TD and CP human movement. The Alpha 1 was shown to be an accurate model of the simplified motion, and exhibited much less movement variation between trials than human research participants.

5.2 Limitations

There are several limitations of the work that has been conducted in this study. Key limitations are:

- The small research participant population size with a narrow age range.
- The PT motion is predominantly isolated around a single axis, so only a two dimensional movement.
- The PT modelled by the Alpha 1 humanoid robot is a simplified version of the real human movement.
- Only the gyroscope data of the WATD has been utilised.

5.3 Future Work

Future work should be done to improve the accuracy of the WATD and to further develop the Alpha 1 humanoid robot as a model for human movement. The following items are planned to be implemented to achieve these goals:

- Miniaturisation of the WATD and fitting of the case to allow the device to be firmly secured as close as possible to the body.
- Increased WATD memory to allow for a longer tracking window or multiple trials to be tracked.
- Adding an audio indication for WATD memory and tracking state to avoid the need for the tester to see the WATD during trials.
- Further development of the edge-computing feature of the system by including analytics in the edge-computer.
- Processing of the WATD accelerometer and magnetometer data for movement trials.
- Analysis of more clinical movements using the Alpha 1 robot, such as other measurement scales or gait.
- Use of the WATD and Alpha 1 to generate training data for a deep-learning neural network based classifier to classify normal and abnormal motions in CP.
- Increase the human population size sampled in this study.

Abbreviations

9DOF	9 degrees of freedom
API	Application programming interface
CP	Cerebral palsy
DAROM	Dynamic evaluation of range of movement
DROM	Range of motion deficit
EX	First swing excursion
FA	First angle
GMFM	Gross Motor Function Measure
I2C	Inter-Integrated
IMU	Inertial measurement unit
IoT	Internet of Things
MAS	Modified Ashworth scale
MCU	Microcontroller unit
MS	Multiple sclerosis
MTS	Modified Tardieu scale
n	Number of swings
PPV	Peak-to-peak angular velocities
R	Cross-correlation
RA	Resting angle
RI	Relaxation index
RMSE	Root-mean-square error
ROM	Range of motion
SA	Starting angle
SD	Spastic diplegia
T	Duration of oscillations
TD	Typically developed
WATD	Wearable activity tracking device

Bibliography

[1] Xsens. Motion Capture. Accessed 16 Oct 2019. [Online]. Available: https://www.xsens.com/motion-capture

[2] Vicon. Blue Trident. Accessed 16 Oct 2019. [Online]. Available: https://www.vicon.com/hardware/blue-trident/

[3] Fitbit. Fitbit premium. Accessed 24 Oct 2019. [Online]. Available: https://www.fitbit.com/au/fitbit-premium

[4] Fitbit. Fitbit Web API Basics. Accessed 24 Oct 2019. [Online]. Available: https://dev.fitbit.com/build/reference/web-api/basics/

[5] N. J. Cooney, K. P. Joshi, and A. S. Minhas, "A wearable internet of things based system with edge computing for real-time human activity tracking," in *2018 5th Asia-Pacific World Congress on Computer Science and Engineering (APWC on CSE)*, Dec 2018, pp. 26–31.

[6] P. Kumari, M. López-Benítez, G. M. Lee, T. Kim, and A. S. Minhas, "Wearable Internet of Things - from human activity tracking to clinical integration," in *2017 39th Annual International Conference of the IEEE Engineering in Medicine and Biology Society (EMBC)*, July 2017, pp. 2361–2364.

[7] D. Giansanti, S. Morelli, G. Maccioni, and G. Costantini, "Toward the design of a wearable system for fall-risk detection in telerehabilitation," *Telemedicine and e-Health*, vol. 15, no. 3, pp. 296–299, 2009, pMID: 19382869. [Online]. Available: https://doi.org/10.1089/tmj.2008.0106

[8] J. Lui, A. Ferrone, Z. Y. Lim, L. Colace, and C. Menon, "A novel wearable for rehabilitation using infrared sensors: A preliminary investigation," in *Bioinformatics and Biomedical Engineering*, I. Rojas and F. Ortuño, Eds. Cham: Springer International Publishing, 2017, pp. 573–583.

[9] S. Patel, H.-S. Park, P. Bonato, L. Chan, and M. Rodgers, "A review of wearable sensors and systems with application in rehabilitation," *Journal of neuroengineering and rehabilitation*, vol. 9, p. 21, 04 2012.

[10] T. Thielgen, F. Foerster, G. Fuchs, A. Hornig, and J. Fahrenberg, "Tremor in parkinson's disease: 24-hr monitoring with calibrated accelerometry," *Electromyography and clinical neurophysiology*, vol. 44, no. 3, p. 137—146, 2004. [Online]. Available: http://europepmc.org/abstract/MED/15125053

[11] R. D. Willmann, G. Lanfermann, P. Saini, A. Timmermans, J. t. Vrugt, and S. Winter, "Home stroke rehabilitation for the upper limbs," in *2007 29th Annual International Conference of the IEEE Engineering in Medicine and Biology Society*, Aug 2007, pp. 4015–4018.

[12] O. Aziz, L. Atallah, B. Lo, M. ElHelw, L. Wang, G. Yang, and A. Darzi, "A pervasive body sensor network for measuring postoperative recovery at home," *Surgical Innovation*, vol. 14, no. 2, pp. 83–90, 2007, pMID: 17558012. [Online]. Available: https://doi.org/10.1177/1553350607302326

[13] H. Jimison, M. Pavel, J. Pavel, and J. Mckanna, "Home monitoring of computer interactions for the early detection of dementia," *Conference proceedings : Annual International Conference of the IEEE Engineering in Medicine and Biology Society. IEEE Engineering in Medicine and Biology Society. Conference*, vol. 6, pp. 4533–6, 02 2004.

[14] J. E. Sasaki, B. Sandroff, M. Bamman, and R. W. Motl, "Motion sensors in multiple sclerosis: Narrative review and update of applications," *Expert Review of Medical Devices*, vol. 14, no. 11, pp. 891–900, 2017, pMID: 28956457. [Online]. Available: https://doi.org/10.1080/17434440.2017.1386550

[15] A. Paraschiv-Ionescu, C. J. Newman, L. Carcreff, C. N. Gerber, S. Armand, and K. Aminian, "Locomotion and cadence detection using a single trunk-fixed accelerometer: validity for children with cerebral palsy in daily life-like conditions," *J Neuroeng Rehabil*, vol. 16, no. 1, p. 24, 2019.

[16] C. Seoyoung and K. Jonghyun, "Improving modified tardieu scale assessment using inertial measurement unit with visual biofeedback," in *Conf Proc IEEE Eng Med Biol Soc*, vol. 2016, 2016, pp. 4703–4706.

[17] A. Szopa, M. Domagalska-Szopa, Z. Kidon, and M. Syczewska, "Quadriceps femoris spasticity in children with cerebral palsy: measurement with the pendulum test and relationship with gait abnormalities," *J Neuroeng Rehabil*, vol. 11, p. 166, 2014.

[18] J. Ko and M. Kim, "Reliability and Responsiveness of the Gross Motor Function Measure-88 in Children With Cerebral Palsy," *Physical Therapy*, vol. 93, no. 3, pp. 393–400, 03 2013. [Online]. Available: https://doi.org/10.2522/ptj.20110374

[19] M. Iosa, T. Marro, S. Paolucci, and D. Morelli, "Stability and harmony of gait in children with cerebral palsy," *Res Dev Disabil*, vol. 33, no. 1, pp. 129–35, 2012.

[20] M. Domagalska, A. Szopa, M. Syczewska, S. Pietraszek, Z. Kidon, and G. Onik, "The relationship between clinical measurements and gait analysis data in children with cerebral palsy," *Gait Posture*, vol. 38, no. 4, pp. 1038–43, 2013.

[21] J. Taborri, E. Scalona, E. Palermo, S. Rossi, and P. Cappa, "Validation of inter-subject training for hidden markov models applied to gait phase detection in children with cerebral palsy," *Sensors (Basel)*, vol. 15, no. 9, pp. 24 514–29, 2015.

[22] A. G. Cutti, A. Ferrari, P. Garofalo, M. Raggi, A. Cappello, and A. Ferrari, "'outwalk': a protocol for clinical gait analysis based on inertial and magnetic sensors," *Medical & Biological Engineering & Computing*, vol. 48, no. 1, p. 17, Nov 2009. [Online]. Available: https://doi.org/10.1007/s11517-009-0545-x

[23] R. Wartenberg, "Pendulousness of the legs as a diagnostic test," *Neurology*, vol. 1, no. 1, pp. 18–18, 1951. [Online]. Available: https://n.neurology.org/content/1/1/18

[24] T. Bajd and L. Vodovnik, "Pendulum testing of spasticity," *Journal of Biomedical Engineering*, vol. 6, no. 1, pp. 9 – 16, 1984. [Online]. Available: http://www.sciencedirect.com/science/article/pii/0141542584900037

[25] UBTECH. (2017) Alpha 1 Pro. Accessed 1 Nov 2018. [Online]. Available: https://ubtrobot.com/pages/alpha

[26] A. Pfister, A. M. West, S. Bronner, and J. A. Noah, "Comparative abilities of microsoft kinect and vicon 3d motion capture for gait analysis," *Journal of Medical Engineering & Technology*, vol. 38, no. 5, pp. 274–280, 2014. [Online]. Available: https://doi.org/10.3109/03091902.2014.909540

[27] J. W. Yoo, D. R. Lee, Y. J. Cha, and S. H. You, "Augmented effects of emg biofeedback interfaced with virtual reality on neuromuscular control and movement coordination during reaching in children with cerebral palsy," *NeuroRehabilitation*, vol. 40, no. 2, pp. 175–185, 2017.

[28] K. Bjornson, C. Zhou, S. Fatone, M. Orendurff, R. Stevenson, and S. Rashid, "The effect of ankle-foot orthoses on community-based walking in cerebral palsy: A clinical pilot study," *Pediatr Phys Ther*, vol. 28, no. 2, pp. 179–86, 2016.

[29] AutoDesk Inventor 2020. AutoDesk, San Rafael, 2019. [Online]. Available: https://www.autodesk.com.au/products/inventor/new-features

[30] FlashForge. (2019) Dreamer. Accessed 14 Oct 2019. [Online]. Available: https://www.flashforge.com/consumer/detail/Dreamer?id=5

[31] MATLAB 2019a. MathWorks, Natick, 2019. [Online]. Available: https://au.mathworks.com/

[32] J. Rodda and H. K. Graham, "Classification of gait patterns in spastic hemiplegia and spastic diplegia: a basis for a management algorithm," *European Journal of Neurology*, vol. 8, no. s5, pp. 98–108, 2001.

[33] P. Kumari, N. J. Cooney, T. Kim, and A. S. Minhas, "Gait analysis in spastic hemiplegia and diplegia cerebral palsy using a wearable activity tracking device – a data quality analysis for deep convolutional neural networks," in Proceedings of *5th Asia-Pacific World Congress on Computer Science and Engineering (APWC on CSE)*, Nadi, Fiji, **Dec 10-12 2018 (accepted)**.

Note: *References [5] and [33] are papers in which I am a co-author. At this time, [33] has not yet been published to the IEEE Xplore Digital Library.*